

REFERENCES

- Allen, J.R.L. (1971). Bed forms due to mass transfer in turbulent flows: a kaleidoscope of phenomena. Journal of Fluid Mechanics, 49(1), 49-63.
- Allen, J.R.L. (1971). Transverse erosional marks of mud and rock: their physical basis and geological significance. Sedimentary Geology, 5, 167-385.
- Azimi, A., Papangelakis, V.G. and Dutrizac, J.E. (2007). Modelling of calcium sulphate solubility in concentrated multi-component sulphate solutions. Fluid Phase Equilibria, 260, 300-315.
- Berger, F.P. and Hau, K. -F. F. -L. (1977). Mass transfer in turbulent pipe flow measured by the electrochemical method. Journal of Heat Mass Transfer, 20, 1185-1194
- Blumberg, P.N. (1970). Flutes: a study of stable, periodic dissolution profiles resulting from the interaction of a soluble surface and an adjacent turbulent flow. PhD thesis, University of Michigan.
- Blumberg, P.N. and Curl R.L. (1974). Experimental and theoretical studies of dissolution roughness. Journal of Fluid Mechanics, 65(4), 735-751.
- Bosbach, D. and Rammensee, W. (1994). In situ investigation of growth and dissolution on the (010) surface of gypsum by Scanning Force Microscopy, Geochimica et Cosmochimica Acta, 58(2), 843-849.
- Broul, M., Nyvlt, J. and Schmel, O. (1981). Solubility in Inorganic Two-Component Systems. New York: Elsevier.
- Burrill, K.A. and Cheluget E.L. (1998). Corrosion of CANDU outlet feeder pipes. Paper presented at the 1998 JAIF International Conference, Japan Atomic Industrial Forum on Water Chemistry in Nuclear Power Plants, October 13-16. Kashiwazaki, Japan.
- Coney, M.W.E., Wilkin, S.J. and Oates, H.S. (1982). Thermal-hydraulic effects on mass transfer behaviour and on erosion-corrosion metal loss rates. EdF (International Specialists' Meeting on Erosion-Corrosion of steels in high temperature water and wet steam, France.
- Curl, R.L. (1974). Deducing flow velocity in cave conduits from scallops. The NSS Bulletin, 36(2), 1-5.

- Ferng Y., Yin-Pang MA. And Kuo-Tong MA. (1999). Flow-assisted corrosion of pipes. Nuclear Technology, 126
- Henderson, E.P. and Perry, S.H. (1958). Studies on siderites. Proc.U.S. Natl. Museum, 107, 339-403.
- James, A.N. and Lupton, A.R.R. (1978). Gypsum and anhydrite in foundations of hydraulic structures. Geotechnique, 28(3), 249-272.
- Jeschke, A.A., Vosbeck, K. and Dreybrodt, W. (2001). Surface controlled dissolution rates of gypsum in aqueous solutions exhibit non linear dissolution kinetics. Geochimica et Cosmochimica Acta, 65(1), 27-34.
- Lebedev, A.L. and Lekhov, A.V. (1989). Dissolution kinetics of natural-gypsum in water at 5-25oC. Moscow University. 6:865-874.
- Leighly, J., (1948). Cuspate surfaces of melting ice and firn. Geograph. Rev., 38:300-306.
- Lertsurasakda, C. (2007). The effect of surface scalloping on flow hydrodynamics and pressure drop. M.S. Thesis, The Petroleum and Petrochemical College, Chulalongkorn University.
- Lister, D.H., Gauthier, P., Goszczynski, J. and Slade, J. (1998). The accelerated corrosion of CANDU primary piping. Paper presented at the 1998 JAIF International Conference, Japan Atomic Industrial Forum on Water Chemistry in Nuclear Power Plants, Sept 7-11.
- Liu, S. and Nancollas, G.H. (1971). The kinetics of dissolution of calcium sulfate dehydrate. Journal of Inorganic Nuclear Chemistry, 33, 2311-2316.
- Marshall, L.W. and Slusher, R. (1975) The ionization constant of nitric acid at high temperatures from solubilities of calcium sulfate in HNO₃-H₂O, 100-350°C; activity coefficients and thermodynamic functions. Journal of Inorganic Nuclear Chemistry, 37, 1191-1202.
- Opdyke, N.B., Gust, G. and Ledwell, R.J. (1987) Mass transfer from smooth alabaster surfaces in turbulent flows. Geophysical research letters, 14(11), 1131-1134.
- Perry H.R. and Green W.D. (1997) Perry's Chemical Engineers' Handbook: Seventh Edition. New York: McGraw-Hill.

- Raines, M. and Dewers, T. (1997) Mixed kinetics control of fluid-rock interaction in reservoir production scenarios. Journal of Petroleum Science and Engineering, 17, 139-155.
- Rechenberg, W. and Sprung, S. (1983) Composition of the solution in the hydration of cement. Cement and Concrete Research, 13, 119-126.
- Shao, Y. (2006) The scalloping phenomenon and the influence of oxygen on flow-accelerated corrosion in feedwater systems. Master of science in engineering thesis, University of New Brunswick.
- Sharp, J.P. (1974) The wolf-creek glaciers, St Elias Range, Yukon Territory. Geograph. Rev., 37, 26-52.
- Villien, B., Zheng, Y. and Lister D.H. (2001) The scalloping phenomenon and its significance in flow assisted-corrosion. Proceedings of the twenty sixth annual CNS-CAN student conference, Toronto (June).
- Villien, B., Zheng, Y. and Lister D.H. (2005) Surface dissolution and the development of scallops. Chem. Eng. Comm., 192, 125-136.
- Way, S.J. and Shayan, A. (1989) Early hydration of a portland cement in water and sodium hydroxide solutions: composition of solutions and nature of solid phases. Cement and Concrete Research, 19, 759-769.

APPENDICES

Appendix A Plaster Test Section Mixing and Molding

Air often gets trapped inside the plaster test sections resulting in non-uniform dissolution of plaster as flow passes over it. From observing and trial-and-error experiments in order to reduce air bubbles inside the plaster test section, it was found that a vacuum pump and separator funnel similar to the system used in previous work had to be employed. However, the molding method was different, since a syringe was used to inject plaster in the liquid state to the acrylic mold to obtain a smoother plaster test section. The ratio between water and plaster was changed from 0.6 in previous work to 0.7 so as to cast a smoother plaster test section. Nevertheless, there was a problem in that the plaster broke easily when being removed from the mold. A releasing agent was used to coat the inside surface of the mold and the steel core but it did not work; in addition, a releasing agent can contaminate the plaster and influence the experiment. Therefore, another technique was used to remove the completed plaster test section instead of using a releasing agent; for example, removing the plaster while still wet after 20 minutes or totally dry after 2 days.

Table A.1 and A.2 shows some results and appearance of the plaster test section from trial and error for several times in each ratio; Figure A.1 shows the plaster test section features in the final step of casting.

Table A.1 The detail of noticeable appearance of plaster test section and procedures in different ratio without coating releasing agent.

R_o	M_{water} (g)	M_{plaster} (g)	Detail (from naked eye)
0.6	300	500	- no well-mixed plaster and deionized water - difficult to inject the plaster liquid into the mold
0.75	300	400	- no smooth plaster - easiest to inject the plaster liquid into the mold
0.725	290	400	- more smooth plaster - easy to inject the plaster liquid into the mold
0.7	280	400	- get the most smooth plaster - easy to inject the plaster liquid into the mold

Notice : - The plaster test section in every case was broken while it was taken out from the acrylic mold.

- The smooth plaster means that the plaster surface has no air bubbles or holes inside.

Table A.2 The detail of noticeable appearance of plaster test section and procedures in different ratio with coating releasing agent.

R_o	M_{water} (g)	M_{plaster} (g)	Detail (from naked eye)
0.75	300	400	- no smooth plaster - many air bubbles spreading surface
0.725	290	400	- more smooth plaster - still get cracking plaster sometime
0.7	280	400	- get the most smooth plaster, no air bubbles inside plaster - seems to take plaster out easily but sometime still get broken plaster

From the experience of molding plaster several times, it can be concluded that the plaster should be mixed with deionized water in a ratio of $R_o = 0.7$. The mixed plaster is injected to the acrylic mold which has a steel rod in the middle. After 20 minutes, the plaster conduit was removed from the mold while still wet. The smooth plaster conduit can be achieved without contamination by a releasing reagent.

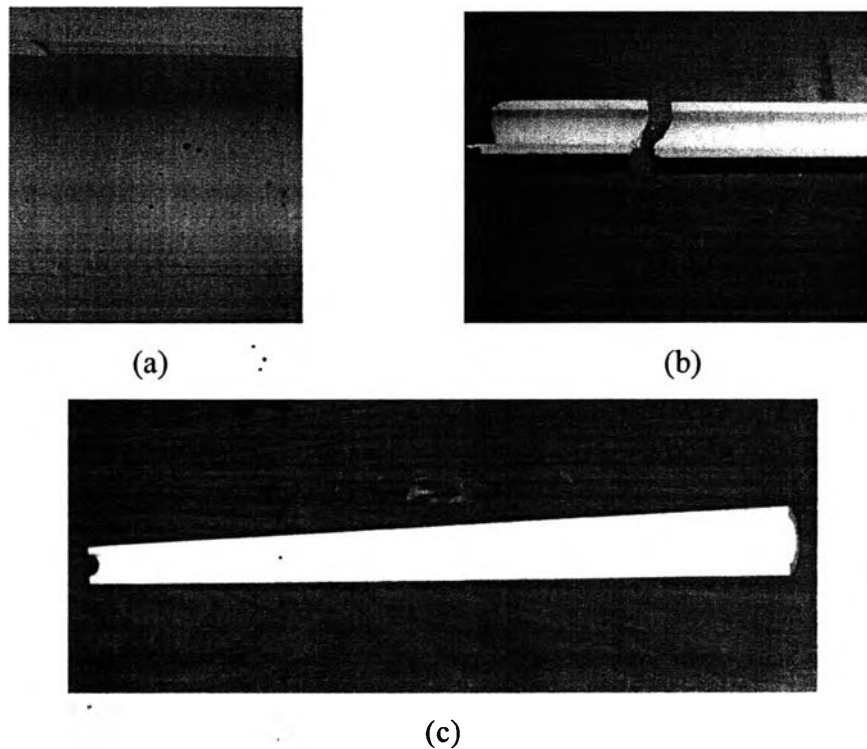


Figure A.1 The plaster test section after casting (a) air bubbles or holes on the surface (b) cracking plaster (c) complete plaster.

Appendix B Solubility of Gypsum

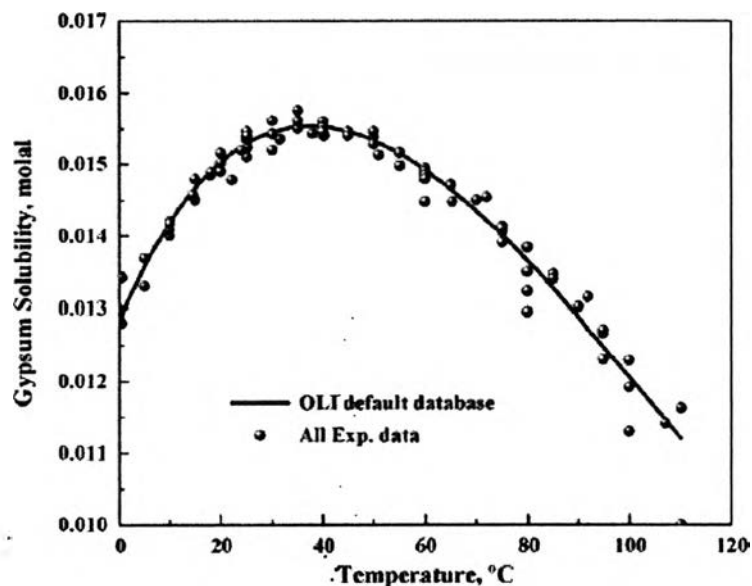


Figure B.1 Dihydrate solubility in H_2O vs. temperature. The curve is determined from the OLI default database (Azimi *et al.*, 2007)

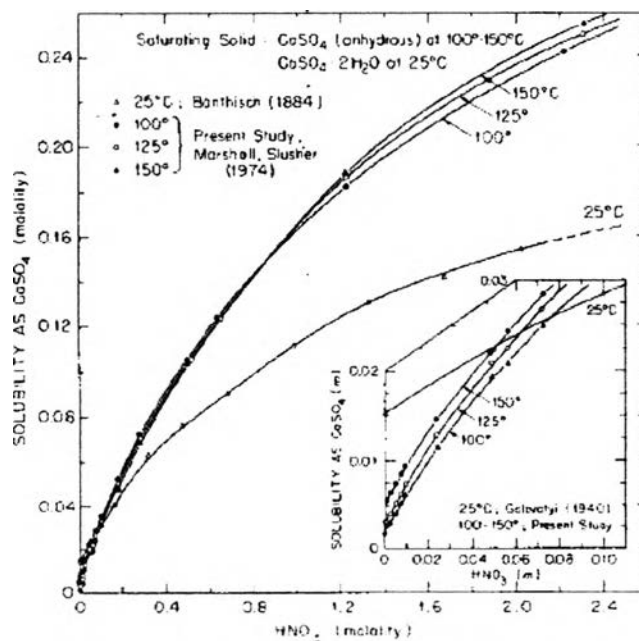


Figure B.2 Molal solubility of $\text{CaSO}_4 \cdot 2\text{H}_2\text{O}$ at 25°C and CaSO_4 (anhydrous) at 100-150°C in HNO_3 - H_2O solutions, 0-2.4 molal (Marshall, *et al.* 1975)

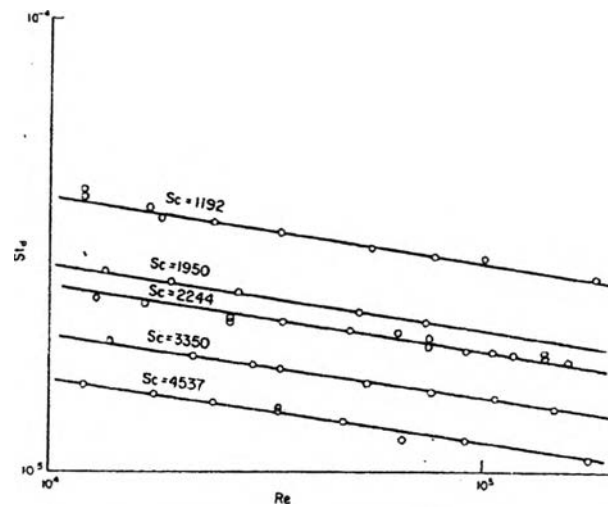


Figure B.3 Stanton number vs Reynolds number in fully developed flow (Schmidt number as parameter) (Berger *et al.*, 1977)

Table B.1 Properties of solutions at different NaOH concentrations and temperatures (Berger *et al.*, 1977)

NaOH (M)	Temp. (°C)	$\mu \times 10^3$ (kg·ms)	$\nu \times 10^6$ (m ² /s)	$D \times 10^{10}$ (m ² /s)	Sc	$\rho \times 10^{-3}$ (kg/m ³)
1.0	20.5	1.22	1.173	6.014	1950	1.04
1.0	30.5	0.97	0.9327	7.822	1192	1.04
2.0	25.5	1.345	1.245	5.548	2244	1.08
2.0	28.0	1.27	1.176	5.925	1985	1.08
2.0	40.0	0.995	0.9123	7.864	1160	1.08
4.0	24.5	2.26	1.948	3.291	5919	1.16
4.0	29.5	1.995	1.72	3.791	4837	1.16
4.0	35.0	1.73	1.491	4.451	3350	1.16

C.2 The Raw Data for Run Experiment under Condition, $\text{pH}_{25^\circ\text{C}}$ 3 and 25°C

Table C.5 Raw data for run at flow rate 25 LPM, $\text{pH}_{25^\circ\text{C}}$ 3 and 25°C (the first run)

Sample (No.)	Calcium concentration from AAS (mg/l)			real Ca conc. (mg/l)	Difference in Ca conc. (mg/l)	Dissolution Rate ($\text{g/m}^2\cdot\text{min}$)
	#1	#2	Average			
0, #1	1.43	1.44	1.44	-	-	-
0, #2	1.43	1.44	1.44	-	-	-
average	1.43	1.44	1.44	35.88	0.00	-
1	1.86	1.86	1.86	37.20	1.33	1.13
2	1.83	1.83	1.83	36.60	0.73	0.62
3	1.84	1.84	1.84	36.80	0.92	0.79
4	1.85	1.84	1.85	36.90	1.03	0.87
5	1.86	1.86	1.86	37.20	1.33	1.13
6	1.87	1.86	1.87	37.30	1.43	1.21
7	1.87	1.86	1.87	37.30	1.43	1.21
8	1.86	1.87	1.87	37.30	1.43	1.21
9	1.87	1.87	1.87	37.40	1.53	1.30
10	1.87	1.87	1.87	37.40	1.53	1.30
average						1.07

Table C.6 Raw data for run at flow rate 25 LPM, pH_{25°C} 3 and 25°C (the second run)

Sample (No.)	Calcium concentration from AAS (mg/l)				real Ca conc. (mg/l)	Difference in Ca conc. (mg/l)	Dissolution Rate (g/m ² ·min)
	#1	#2	#3	Average			
0, #1	1.37	1.36	1.33	1.35	-	-	-
0, #2	1.39	1.38	1.32	1.36	-	-	-
average	1.38	1.37	1.33	1.36	33.96	0.00	-
1	1.78	1.76	1.75	1.76	35.27	1.31	1.11
2	1.76	1.73	1.74	1.74	34.87	0.91	0.77
3	1.76	1.74	1.74	1.75	34.93	0.98	0.83
4	1.78	1.74	1.72	1.75	34.93	0.98	0.83
5	1.78	1.76	1.72	1.75	35.07	1.11	0.94
6	1.78	1.77	1.72	1.76	35.13	1.18	1.00
7	1.82	1.79	1.74	1.78	35.67	1.71	1.45
8	1.81	1.80	1.74	1.78	35.67	1.71	1.45
9	1.79	1.79	1.75	1.78	35.53	1.58	1.34
10	1.80	1.80	1.75	1.78	35.67	1.71	1.45
average							1.12

Table C.7 Raw data for run at flow rate 35 LPM, pH_{25°C} 3 and 25°C (the first run)

Sample (No.)	Calcium concentration from AAS (mg/l)			real Ca conc. (mg/l)	Difference in Ca conc. (mg/l)	Dissolution Rate (g/m ² ·min)
	#1	#2	Average			
0, #1	1.39	1.36	1.38	-	-	-
0, #2	1.38	1.39	1.39	-	-	-
average	1.39	1.38	1.38	34.50	0.00	-
1	1.80	1.78	1.79	35.80	1.30	1.55
2	1.78	1.77	1.78	35.50	1.00	1.19
3	1.78	1.77	1.78	35.50	1.00	1.19
4	1.78	1.78	1.78	35.60	1.10	1.31
5	1.79	1.77	1.78	35.60	1.10	1.31
6	1.80	1.79	1.80	35.90	1.40	1.66
7	1.81	1.8	1.81	36.10	1.60	1.90
8	1.80	1.8	1.80	36.00	1.50	1.78
9	1.80	1.8	1.80	36.00	1.50	1.78
10	1.81	1.8	1.81	36.10	1.60	1.90
average						1.56

Table C.8 Raw data for run at flow rate 35 LPM, pH_{25°C} 3 and 25°C (the second run)

Sample (No.)	Calcium concentration from AAS (mg/l)				real Ca conc. (mg/l)	Difference in Ca conc. (mg/l)	Dissolution Rate (g/m ² ·min)
	#1	#2	#3	Average			
0, #1	1.41	1.45	1.45	1.44	-	-	-
0, #2	1.44	1.45	1.45	1.45	-	-	-
average	1.43	1.45	1.45	1.44	36.04	0.00	-
1	1.84	1.88	1.88	1.87	37.33	1.29	1.54
2	1.80	1.85	1.84	1.83	36.73	0.69	0.82
3	1.81	1.83	1.83	1.82	36.60	0.56	0.66
4	1.81	1.83	1.83	1.82	36.60	0.56	0.66
5	1.81	1.87	1.87	1.85	37.00	0.96	1.14
6	1.84	1.91	1.91	1.89	37.67	1.63	1.93
7	1.87	1.90	1.91	1.89	37.80	1.76	2.09
8	1.87	1.90	1.92	1.90	37.93	1.89	2.25
9	1.91	1.91	1.92	1.91	38.07	2.03	2.41
10	1.90	1.90	1.91	1.90	38.00	1.96	2.33
average							1.58

C.3 The Raw Data for Run Experiment under Condition, $\text{pH}_{25^\circ\text{C}}$ 10 and 25°C

Table C.9 Raw data for run at flow rate 25 LPM, $\text{pH}_{25^\circ\text{C}}$ 10 and 25°C (the first run)

Sample (No.)	Calcium concentration from AAS (mg/l)	real Ca conc. (mg/l)	Difference in Ca conc. (mg/l)	Dissolution Rate ($\text{g}/\text{m}^2\cdot\text{min}$)
0, #1	0.76	-	-	-
0, #2	0.74	-	-	-
average	0.75	18.70	0.00	-
1	1.04	20.80	2.10	1.78
2	0.98	19.60	0.90	0.76
3	0.98	19.60	0.90	0.76
4	0.97	19.40	0.70	0.59
5	0.97	19.40	0.70	0.59
6	0.96	19.20	0.50	0.42
7	0.96	19.20	0.50	0.42
8	0.98	19.60	0.90	0.76
9	0.96	19.20	0.50	0.42
10	0.98	19.60	0.90	0.76
average				0.73

Table C.10 Raw data for run at flow rate 25 LPM, $\text{pH}_{25^\circ\text{C}}$ 10 and 25°C (the second run)

Sample (No.)	Calcium concentration from AAS (mg/l)				real Ca conc. (mg/l)	Difference in Ca conc. (mg/l)	Dissolution Rate ($\text{g/m}^2\cdot\text{min}$)
	#1	#2	#3	Average			
0, #1	0.68	0.68	0.65	0.67	-	-	-
0, #2	0.66	0.68	0.63	0.66	-	-	-
average	0.67	0.68	0.64	0.66	16.58	0.00	-
1	0.96	0.97	0.96	0.96	19.27	2.68	2.28
2	0.94	0.95	0.93	0.94	18.80	2.22	1.88
3	0.85	0.85	0.83	0.84	16.87	0.28	0.24
4	0.84	0.83	0.84	0.84	16.73	0.15	0.13
5	0.84	0.84	0.83	0.84	16.73	0.15	0.13
6	0.84	0.86	0.82	0.84	16.80	0.22	0.18
7	0.87	0.86	0.84	0.86	17.13	0.55	0.47
8	0.88	0.87	0.85	0.87	17.33	0.75	0.64
9	0.85	0.85	0.85	0.85	17.00	0.42	0.35
10	0.85	0.86	0.85	0.85	17.07	0.48	0.41
average							0.67

Table C.11 Raw data for run at flow rate 35 LPM, $\text{pH}_{25^\circ\text{C}}$ 10 and 25°C

Sample (No.)	Calcium concentration from AAS (mg/l)			real Ca conc. (mg/l)	Difference in Ca conc. (mg/l)	Dissolution Rate ($\text{g/m}^2\cdot\text{min}$)
	#1	#2	Average			
0, #1	0.66	0.67	0.67	-	-	-
0, #2	0.65	0.66	0.66	-	-	-
average	0.66	0.67	0.66	16.60	0.00	-
1	0.95	0.94	0.95	18.90	2.30	2.73
2	0.92	0.92	0.92	18.40	1.80	2.14
3	0.87	0.89	0.88	17.60	1.00	1.19
4	0.88	0.89	0.89	17.70	1.10	1.31
5	0.88	0.87	0.88	17.50	0.90	1.07
6	0.88	0.89	0.89	17.70	1.10	1.31
7	0.87	0.87	0.87	17.40	0.80	0.95
8	0.88	0.86	0.87	17.40	0.80	0.95
9	0.88	0.87	0.88	17.50	0.90	1.07
10	0.87	0.89	0.88	17.60	1.00	1.19
average						1.39

Table C.13 Raw data for run at flow rate 25 LPM, pH_{25°C} 7 and 10°C (the second run)

Sample (No.)	Calcium concentration from AAS (mg/l)				real Ca conc. (mg/l)	Difference in Ca conc. (mg/l)	Dissolution Rate (g/m ² ·min)
	#1	#2	#3	Average			
0, #1	1.36	1.34	1.34	1.35	-	-	-
0, #2	1.35	1.35	1.34	1.35	-	-	-
average	1.36	1.35	1.34	1.35	33.67	0.00	-
1	1.72	1.73	1.71	1.72	34.40	0.73	0.62
2	1.71	1.71	1.71	1.71	34.20	0.53	0.45
3	1.71	1.71	1.71	1.71	34.20	0.53	0.45
4	1.72	1.71	1.71	1.71	34.27	0.60	0.51
5	1.72	1.72	1.72	1.72	34.40	0.73	0.62
6	1.73	1.72	1.71	1.72	34.40	0.73	0.62
7	1.73	1.70	1.71	1.71	34.27	0.60	0.51
8	1.73	1.70	1.71	1.71	34.27	0.60	0.51
9	1.73	1.71	1.72	1.72	34.40	0.73	0.62
10	1.73	1.70	1.71	1.71	34.27	0.60	0.51
average							0.54

Table C.14 Raw data for run at flow rate 35 LPM, pH_{25°C} 7 and 10°C (the first run)

Sample (No.)	Calcium concentration from AAS (mg/l)			real Ca conc. (mg/l)	Difference in Ca conc. (mg/l)	Dissolution Rate (g/m ² ·min)
	#1	#2	Average			
0, #1	1.36	1.36	1.36	-	-	-
0, #2	1.36	1.35	1.36	-	-	-
average	1.36	1.36	1.36	33.94	0.00	-
1	1.72	1.72	1.72	34.40	0.46	0.55
2	1.71	1.72	1.72	34.30	0.36	0.43
3	1.72	1.73	1.73	34.50	0.56	0.67
4	1.72	1.72	1.72	34.40	0.46	0.55
5	1.73	1.72	1.73	34.50	0.56	0.67
6	1.73	1.73	1.73	34.60	0.66	0.79
7	1.73	1.73	1.73	34.60	0.66	0.79
8	1.73	1.74	1.74	34.70	0.76	0.91
9	1.74	1.74	1.74	34.80	0.86	1.03
10	1.73	1.74	1.74	34.70	0.76	0.91
average						0.73

Table C.15 Raw data for run at flow rate 35 LPM, pH_{25°C} 7 and 10°C (the second run)

Sample (No.)	Calcium concentration from AAS (mg/l)				real Ca conc. (mg/l)	Difference in Ca conc. (mg/l)	Dissolution Rate (g/m ² ·min)
	#1	#2	#3	Average			
0, #1	1.39	1.38	1.29	1.35	-	-	-
0, #2	1.30	1.39	1.30	1.33	-	-	-
average	1.35	1.39	1.30	1.34	33.54	0.00	-
1	1.72	1.73	1.65	1.70	34.00	0.46	0.54
2	1.71	1.74	1.66	1.70	34.07	0.52	0.62
3	1.71	1.72	1.65	1.69	33.87	0.32	0.39
4	1.72	1.71	1.65	1.69	33.87	0.32	0.39
5	1.71	1.75	1.66	1.71	34.13	0.59	0.70
6	1.73	1.75	1.67	1.72	34.33	0.79	0.94
7	1.73	1.74	1.67	1.71	34.27	0.72	0.86
8	1.74	1.74	1.68	1.72	34.40	0.86	1.02
9	1.72	1.75	1.68	1.72	34.33	0.79	0.94
10	1.72	1.75	1.69	1.72	34.40	0.86	1.02
average							0.74

Table C.19 Raw data for run at flow rate 35 LPM, $\text{pH}_{25^\circ\text{C}}$ 3 and 10°C (the second run)

Sample (No.)	Calcium concentration from AAS (mg/l)				real Ca conc. (mg/l)	Difference in Ca conc. (mg/l)	Dissolution Rate ($\text{g}/\text{m}^2\cdot\text{min}$)
	#1	#2	#3	Average			
0, #1	1.38	1.38	1.37	1.38	-	-	-
0, #2	1.38	1.37	1.37	1.37	-	-	-
average	1.38	1.38	1.37	1.38	34.38	0.00	-
1	1.41	1.42	1.41	1.41	35.33	0.96	1.14
2	1.40	1.39	1.39	1.39	34.83	0.46	0.54
3	1.41	1.40	1.39	1.40	35.00	0.62	0.74
4	1.41	1.39	1.40	1.40	35.00	0.62	0.74
5	1.41	1.41	1.40	1.41	35.17	0.79	0.94
6	1.41	1.40	1.40	1.40	35.08	0.71	0.84
7	1.40	1.41	1.40	1.40	35.08	0.71	0.84
8	1.41	1.41	1.40	1.41	35.17	0.79	0.94
9	1.41	1.42	1.40	1.41	35.25	0.88	1.04
10	1.42	1.41	1.40	1.41	35.25	0.88	1.04
average							0.88

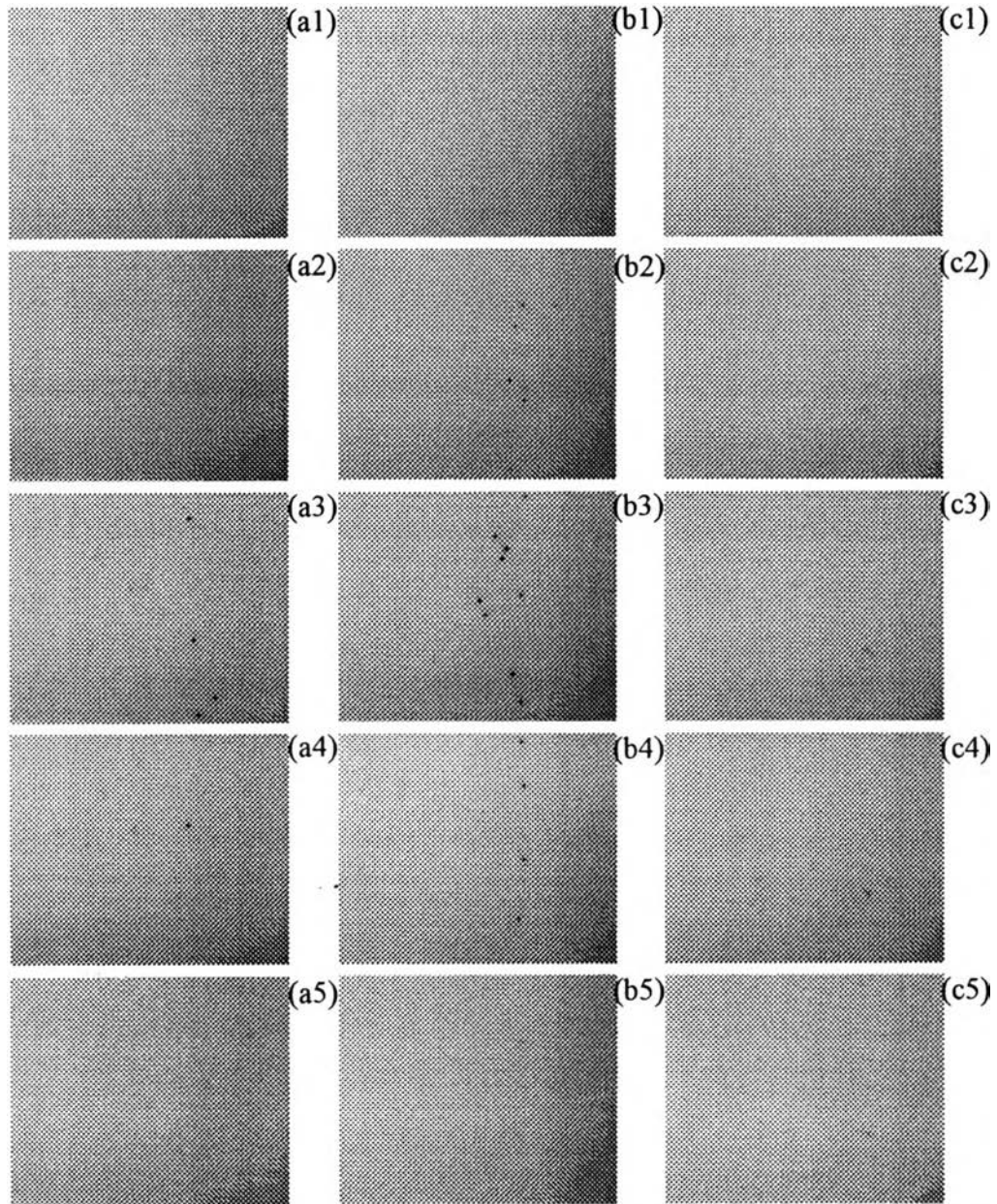
Appendix D The Development of Scallops with Time

Figure D.1 The scallop surface development at every hour at 25 LPM and 10°C under different conditions: (a1-5) $\text{pH}_{25^\circ\text{C}}$ 3, (b1-5) $\text{pH}_{25^\circ\text{C}}$ 7 and (c1-5) $\text{pH}_{25^\circ\text{C}}$ 10

Appendix E The Results from SEM/EDX

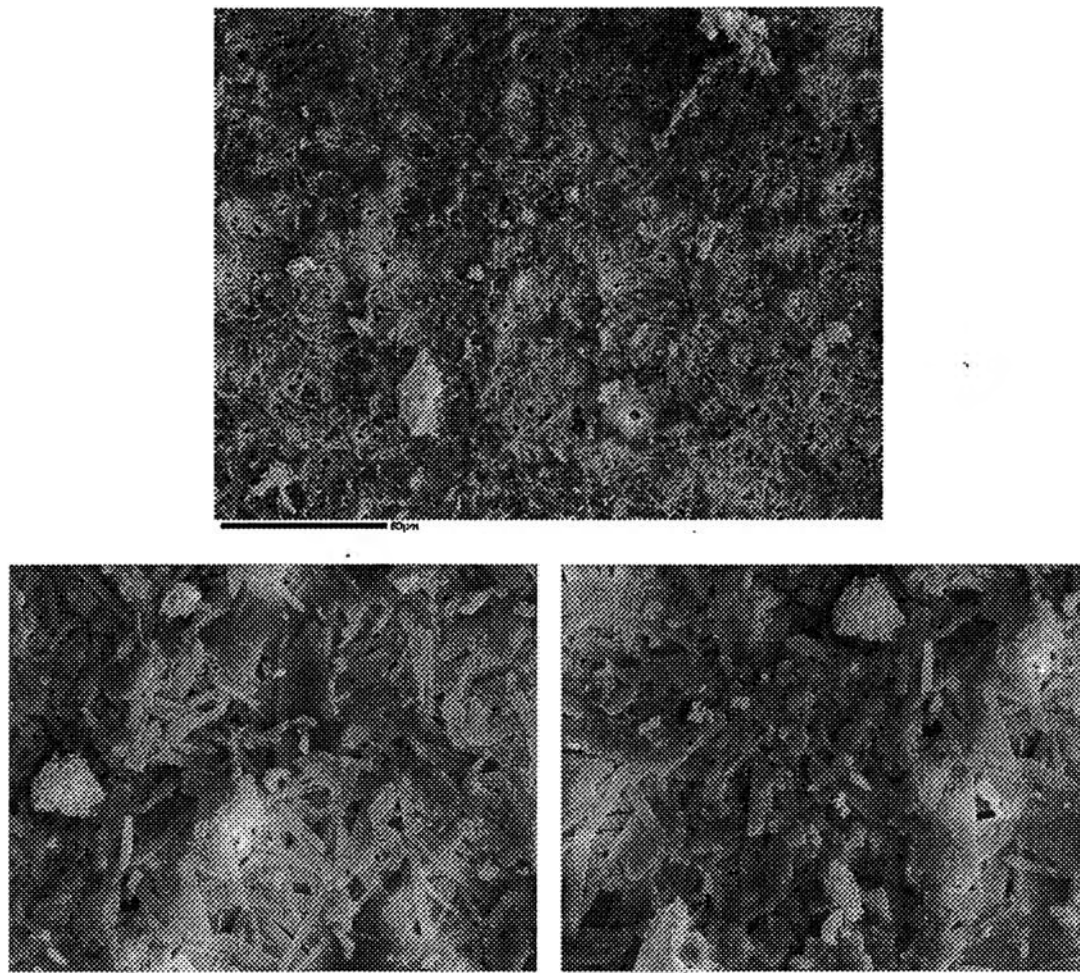


Figure E.1 The SEM images for the plaster conduit before run

Table E.1 The composition of plaster before run

Test Area	Na ₂ O	MgO	Al ₂ O ₃	SiO ₂	SO ₃	ClO ₀	K ₂ O	CaO	FeO	Total
1	0.17	0.19	0.79	0.28	44.71	0.24	0.09	32.83	0.83	80.13
2	0.09	0.07	0.14	0.29	47.52	0.15	0.05	34.37	0	82.68
3	4.08	0.71	12.5	0.62	16.85	3.36	0.07	31.04	13.4	82.61
Ave.	1.45	0.32	4.49	0.40	36.36	1.25	0.07	32.75	4.73	81.81

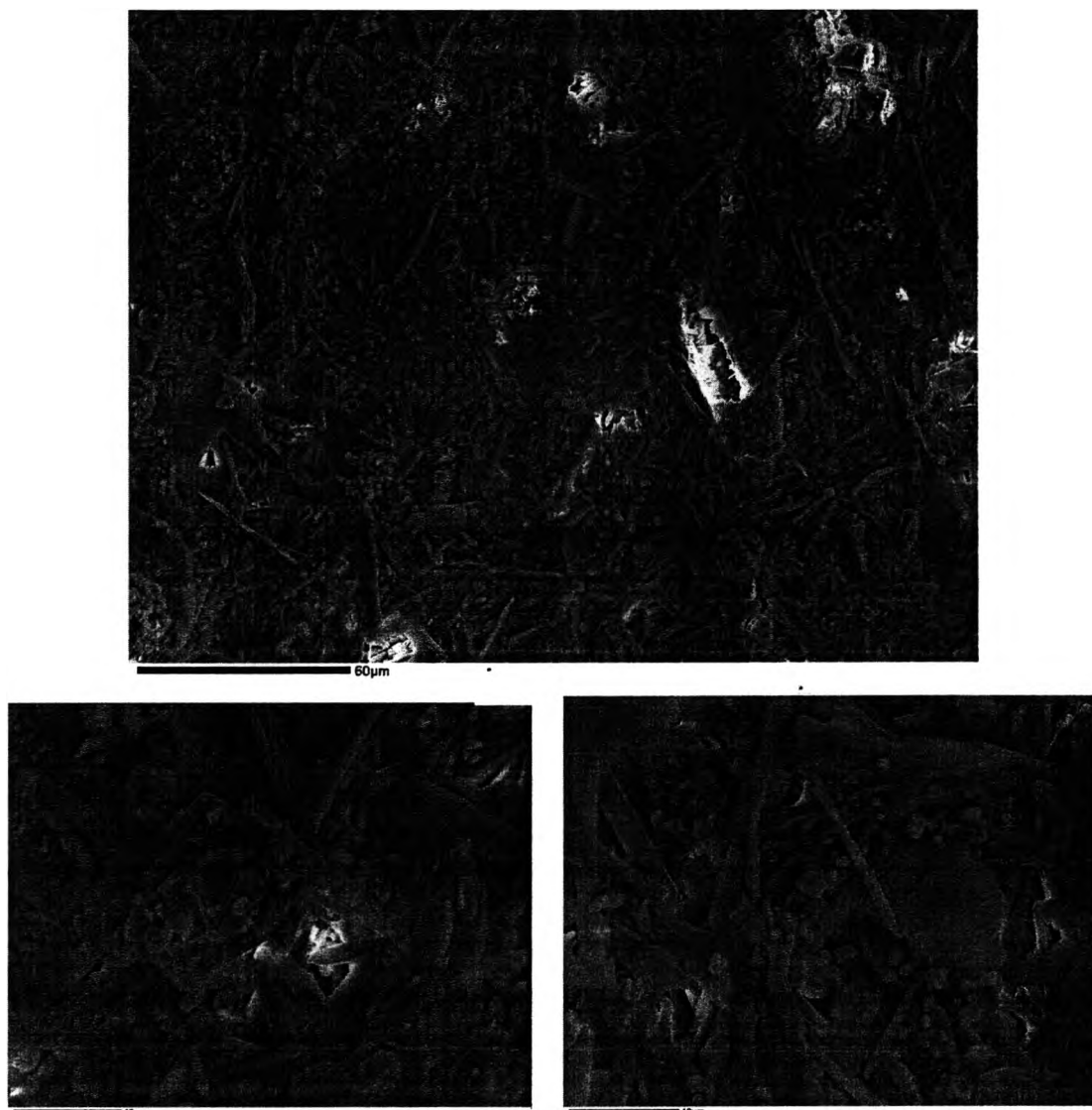


Figure E.2 The SEM images for the plaster conduit after run under 25 LPM, pH_{25°C} 10 and 25°C

Table E.2 The composition of plaster after run under 25 LPM, pH_{25°C} 10 and 25°C

Test Area	Na ₂ O	MgO	Al ₂ O ₃	SiO ₂	SO ₃	ClO ₀	K ₂ O	CaO	FeO	Total
1	0.2	7.99	0.97	2.32	18.19	0.02	0.39	31.81	0.65	62.52
2	0.1	1.21	0.74	1.59	37.6	0	0.21	30.33	0.07	71.84
Ave.	0.15	4.60	0.86	1.96	27.90	0.01	0.30	31.07	0.36	67.18

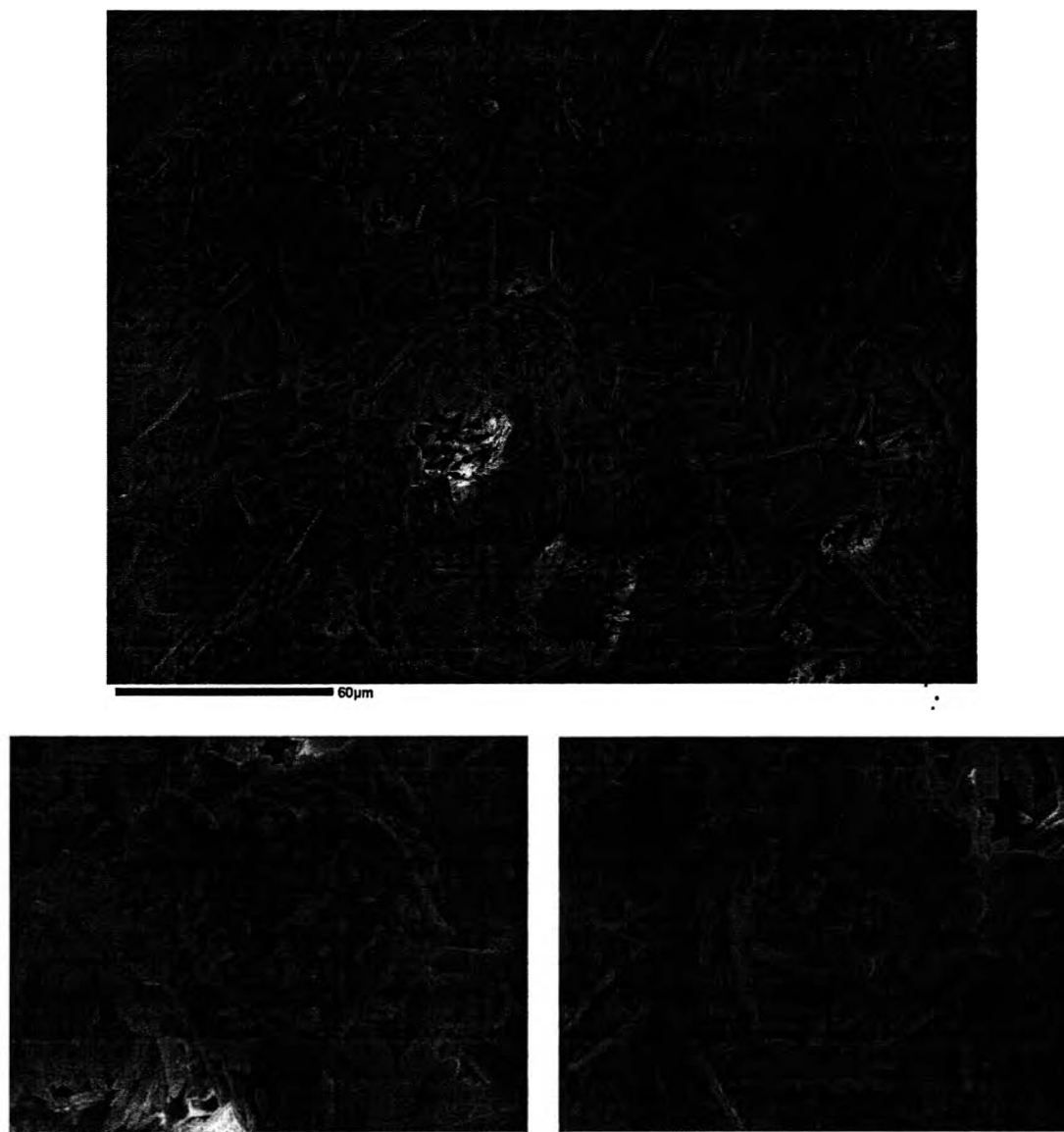


Figure E.3 The SEM images for the plaster conduit after run under 35 LPM, $\text{pH}_{25^\circ\text{C}}$ 7 and 25°C

Table E.3 The composition of plaster after run under 35 LPM, $\text{pH}_{25^\circ\text{C}}$ 7 and 25°C

Test Area	Na ₂ O	MgO	Al ₂ O ₃	SiO ₂	SO ₃	ClO ₀	K ₂ O	CaO	FeO	Total
1	0.09	2.88	1.5	9.68	22.94	0.05	0.47	23.76	1.34	62.73
2	0.45	14.71	9.44	14.75	1.28	0.15	2.16	24.33	0.76	68.04
3	0.48	26.36	0.58	1.05	0.76	0.03	0.05	33.26	0.05	62.62
Ave.	0.34	14.65	3.84	8.49	8.33	0.08	0.89	27.12	0.72	64.46

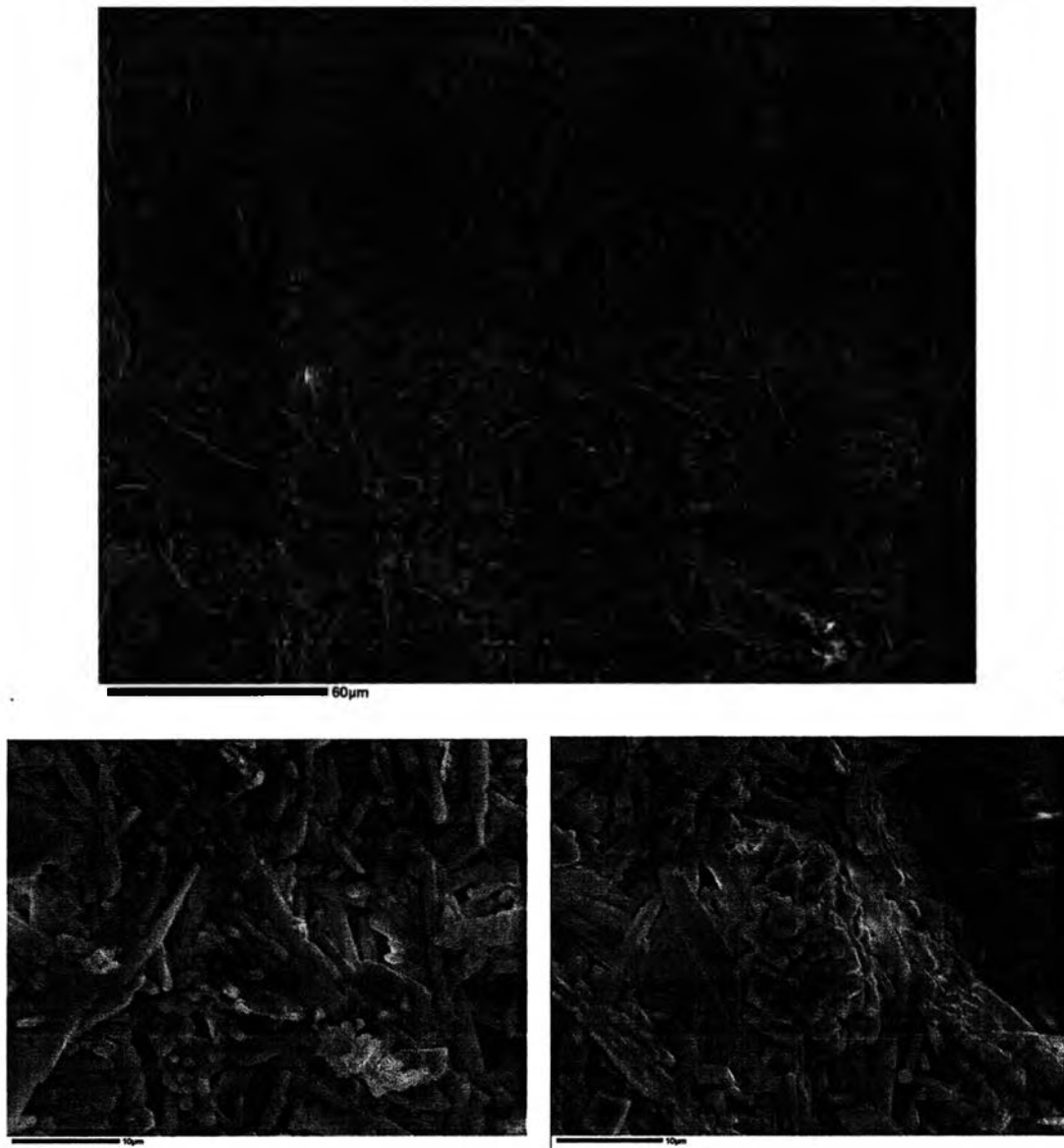


Figure E.4 The SEM images for the plaster conduit after run under 25 LPM, pH_{25°C} 3 and 25°C

Table E.4 The composition of plaster after run under 25 LPM, pH_{25°C} 3 and 25°C

Test Area	Na ₂ O	MgO	Al ₂ O ₃	SiO ₂	SO ₃	ClO ₀	K ₂ O	CaO	FeO	Total
1	0.09	1.6	0.98	2.54	30.1	0	0.30	26.2	0.41	62.2
2	0.09	2.46	1.21	2.85	35.3	0	0.35	28.5	0.17	71.0
3	0.03	4.46	0.78	1.81	26.6	0.02	0.27	28.4	0	62.4
Ave.	0.07	2.84	0.99	2.40	30.69	0.01	0.31	27.69	0.19	65.19

Appendix F Dissolution Rate Along the Pipe and Dissolution Coefficient

F.1 Dissolution Rate Along the Pipe

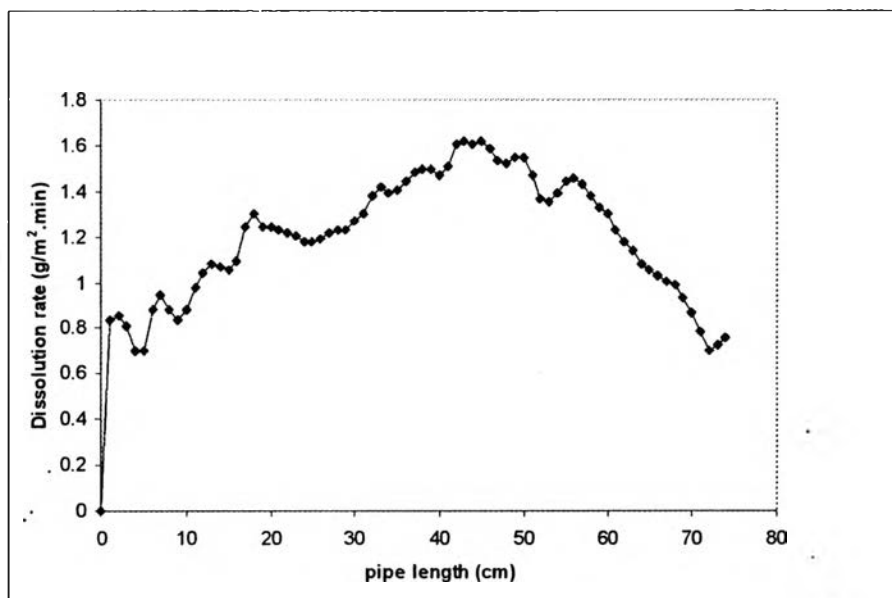


Figure F.1 The dissolution rate profile along the pipe under condition pH_{25°C} 3, 25°C and 25 LPM (the second run)

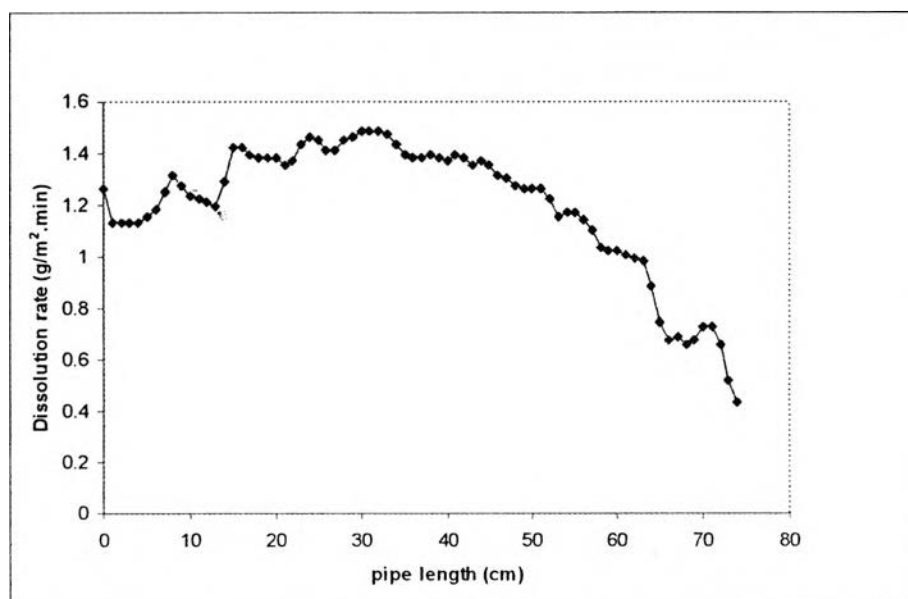


Figure F.2 The dissolution rate profile along the pipe under condition pH_{25°C} 7, 25°C and 25 LPM (the second run)

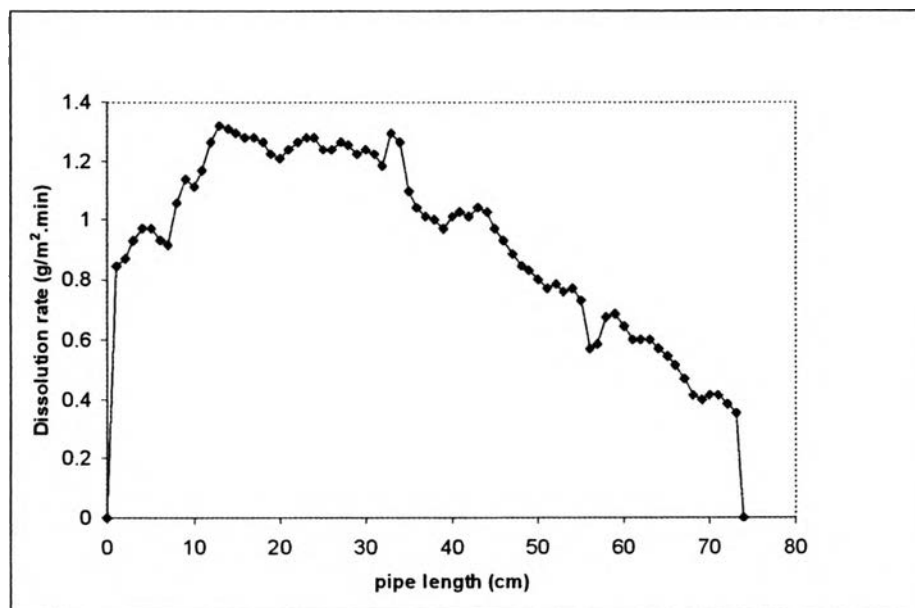


Figure F.3 The dissolution rate profile along the pipe under condition $\text{pH}_{25^\circ\text{C}} 10$, 25°C and 25 LPM (the second run)

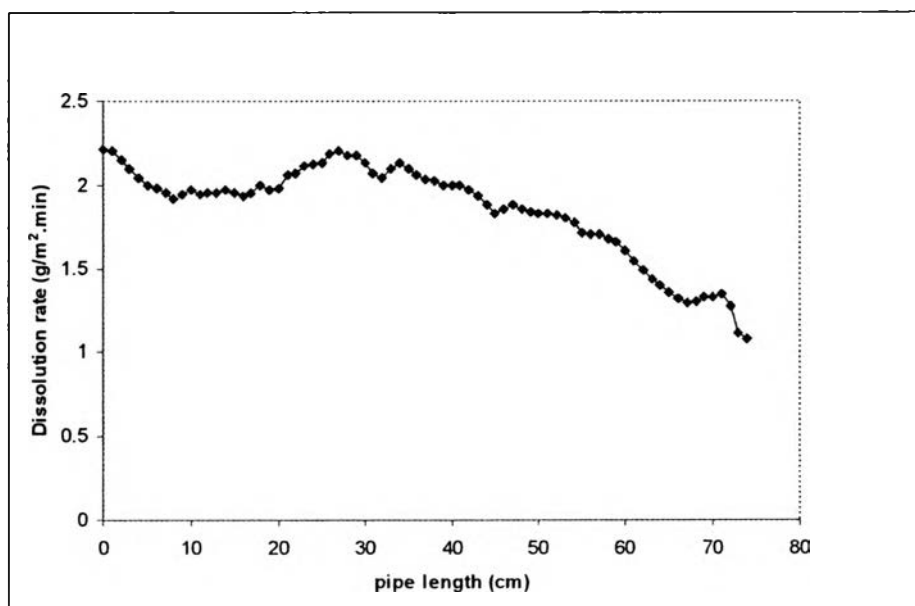


Figure F.4 The dissolution rate profile along the pipe under condition $\text{pH}_{25^\circ\text{C}} 3$, 25°C and 35 LPM (the first run)

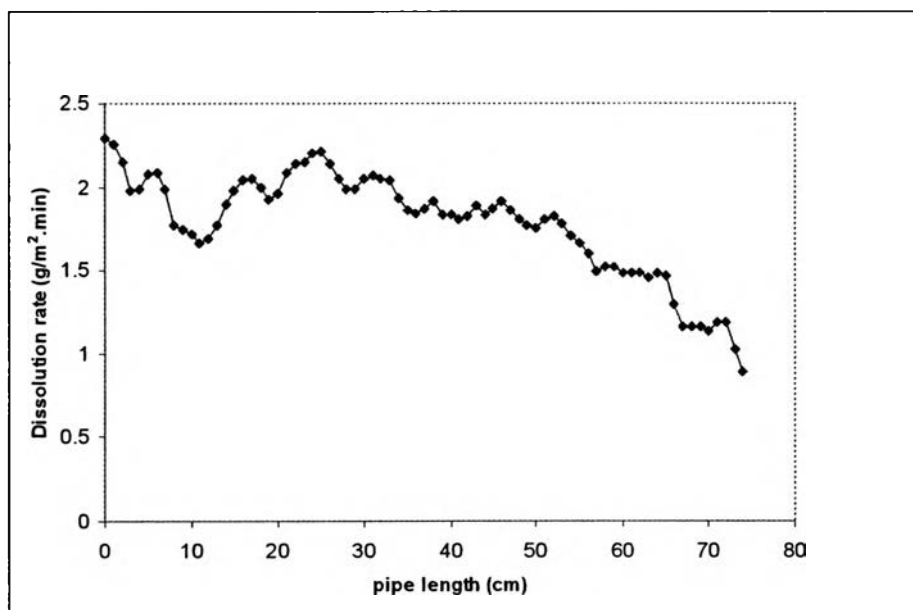


Figure F.5 The dissolution rate profile along the pipe under condition $\text{pH}_{25^\circ\text{C}} 3$, 25°C and 35 LPM (the second run)

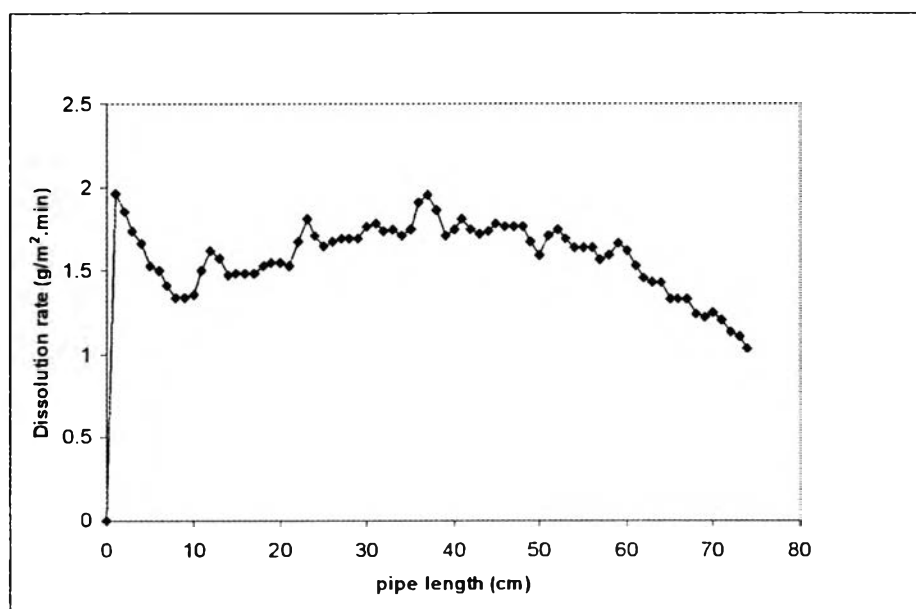


Figure F.6 The dissolution rate profile along the pipe under condition $\text{pH}_{25^\circ\text{C}} 7$, 25°C and 35 LPM (the first run)

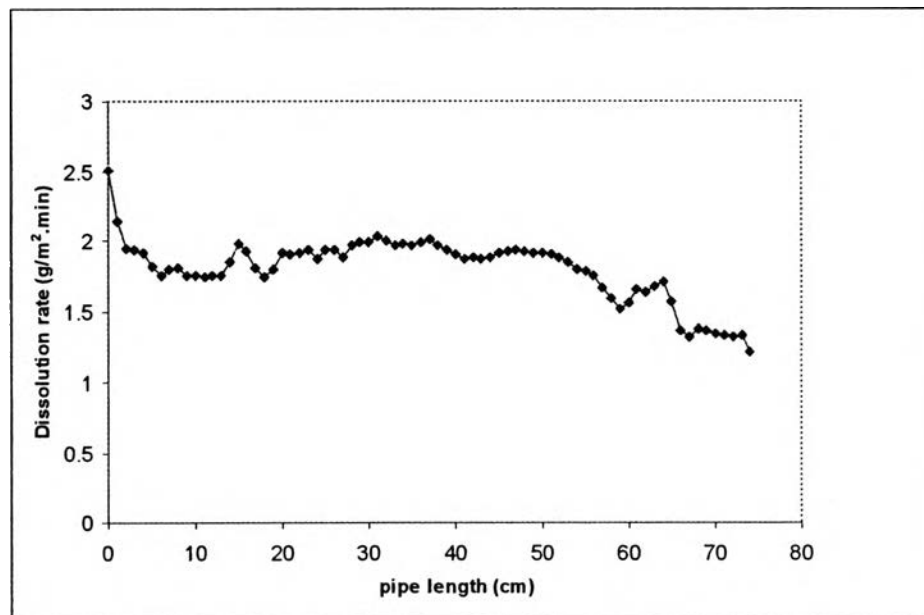


Figure F.7 The dissolution rate profile along the pipe under condition $\text{pH}_{25^{\circ}\text{C}} 7$, 25°C and 35 LPM (the second run)

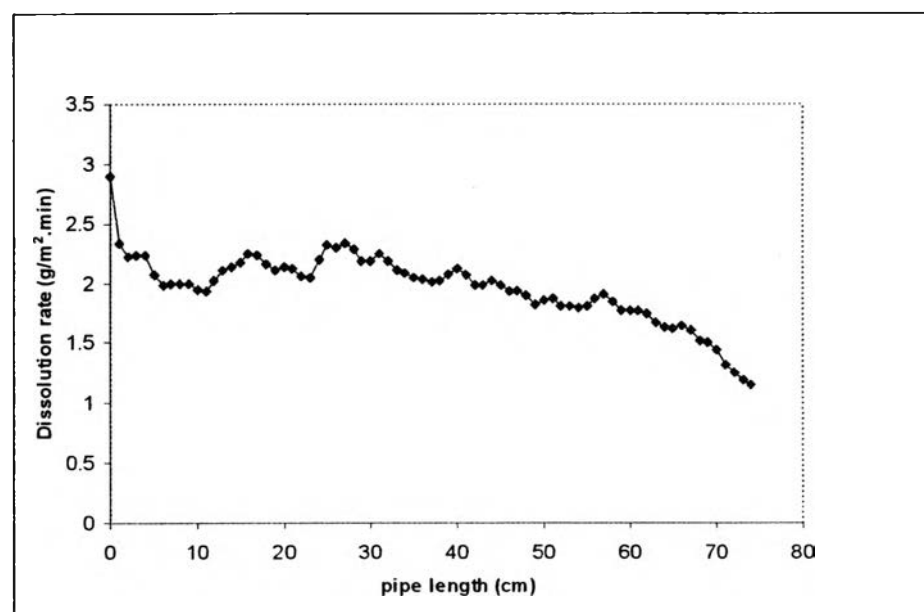


Figure F.8 The dissolution rate profile along the pipe under condition $\text{pH}_{25^{\circ}\text{C}} 10$, 25°C and 35 LPM (the first run)

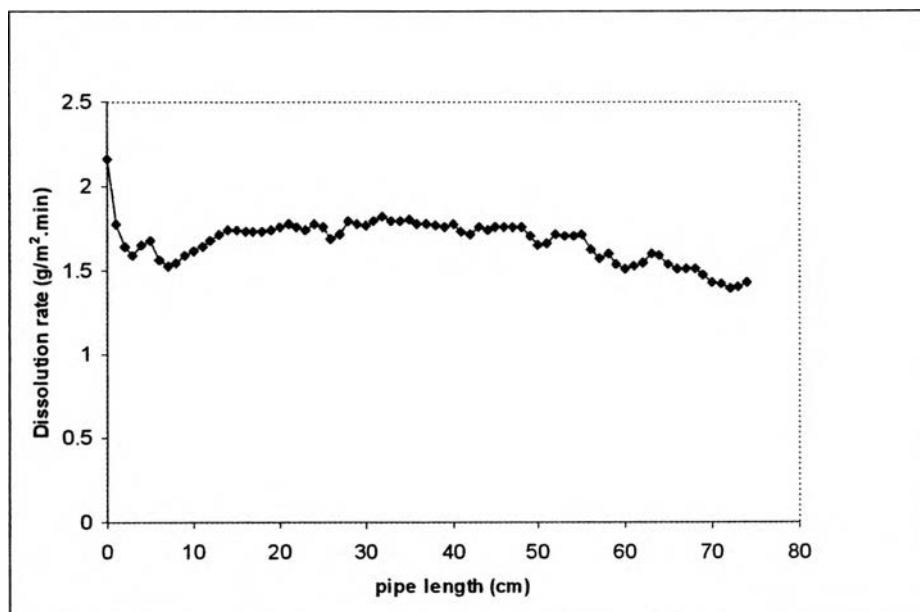


Figure F.9 The dissolution rate profile along the pipe under condition $\text{pH}_{25^\circ\text{C}} 10$, 25°C and 35 LPM (the second run)

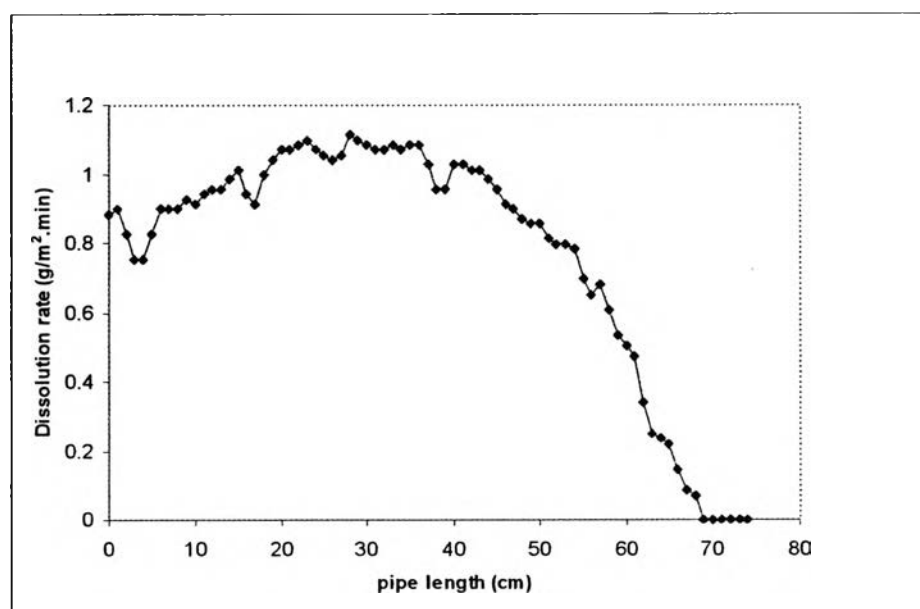


Figure F.10 The dissolution rate profile along the pipe under condition $\text{pH}_{25^\circ\text{C}} 3$, 10°C and 25 LPM (the second run)

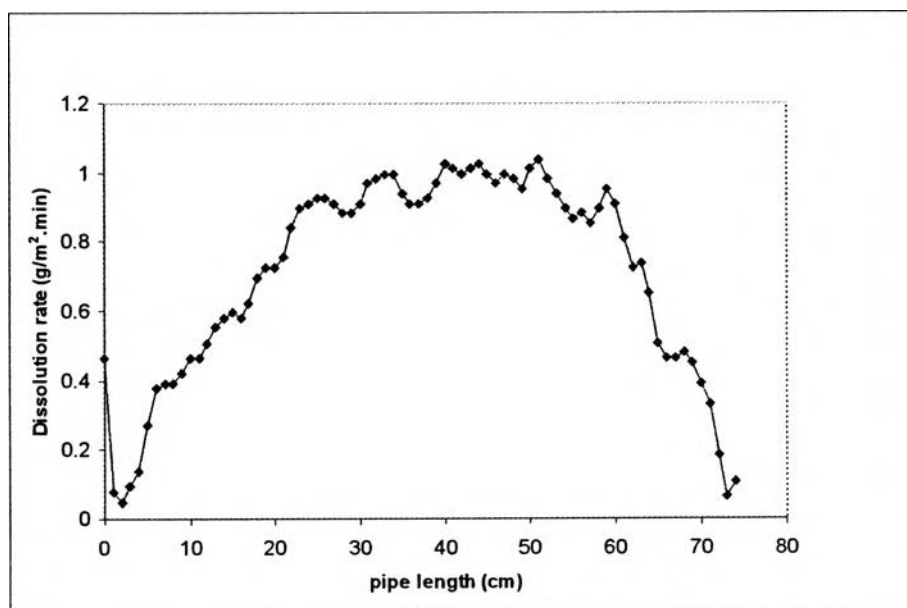


Figure F.11 The dissolution rate profile along the pipe under condition $\text{pH}_{25^\circ\text{C}} 7$, 10°C and 25 LPM (the second run)

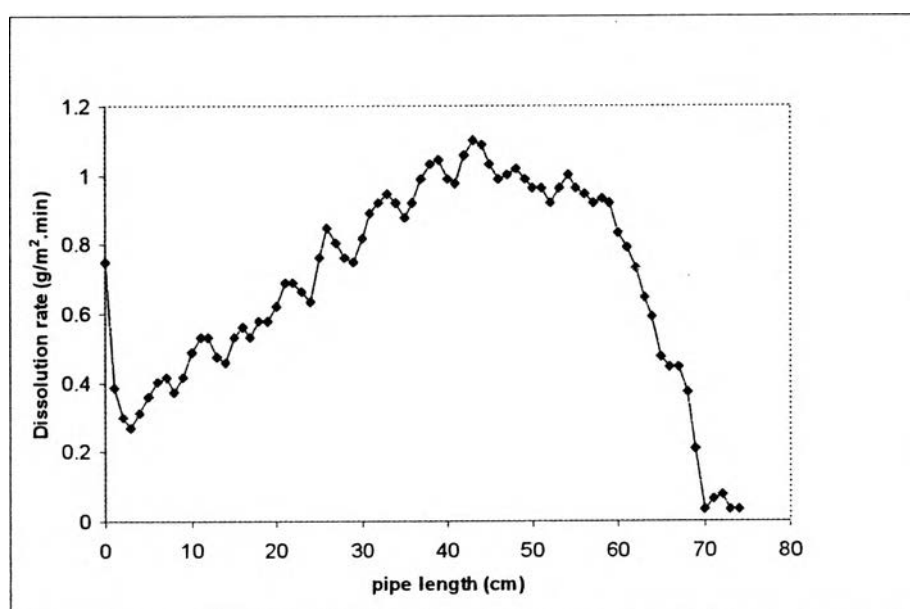


Figure F.12 The dissolution rate profile along the pipe under condition $\text{pH}_{25^\circ\text{C}} 10$, 10°C and 25 LPM (the second run)

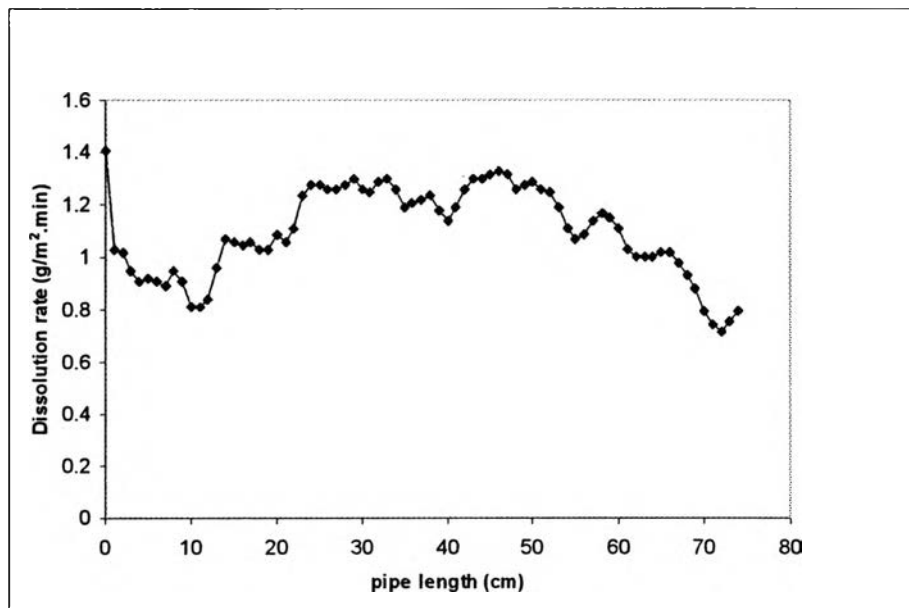


Figure F.13 The dissolution rate profile along the pipe under condition $\text{pH}_{25^\circ\text{C}} 3$, 10°C and 35 LPM (the first run)

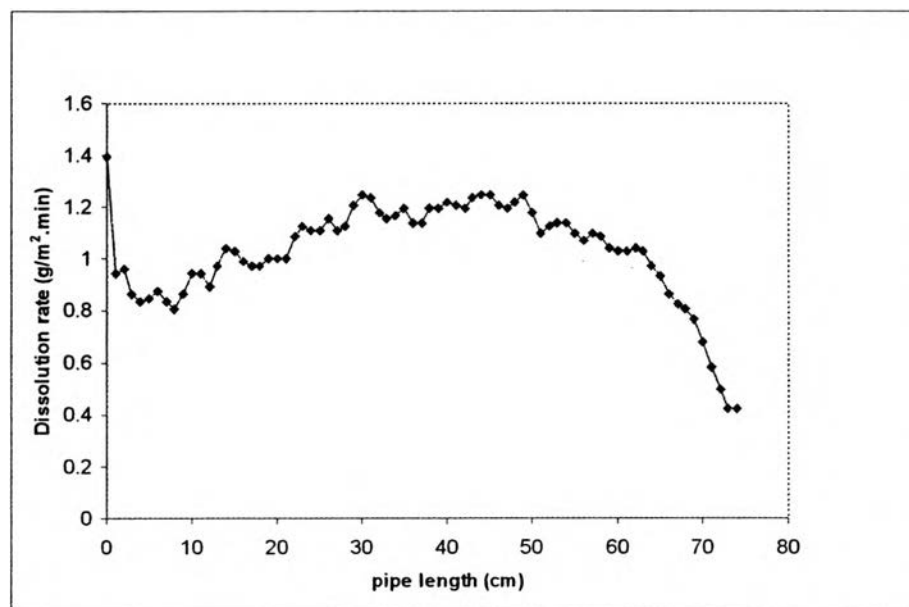


Figure F.14 The dissolution rate profile along the pipe under condition $\text{pH}_{25^\circ\text{C}} 3$, 10°C and 35 LPM (the second run)

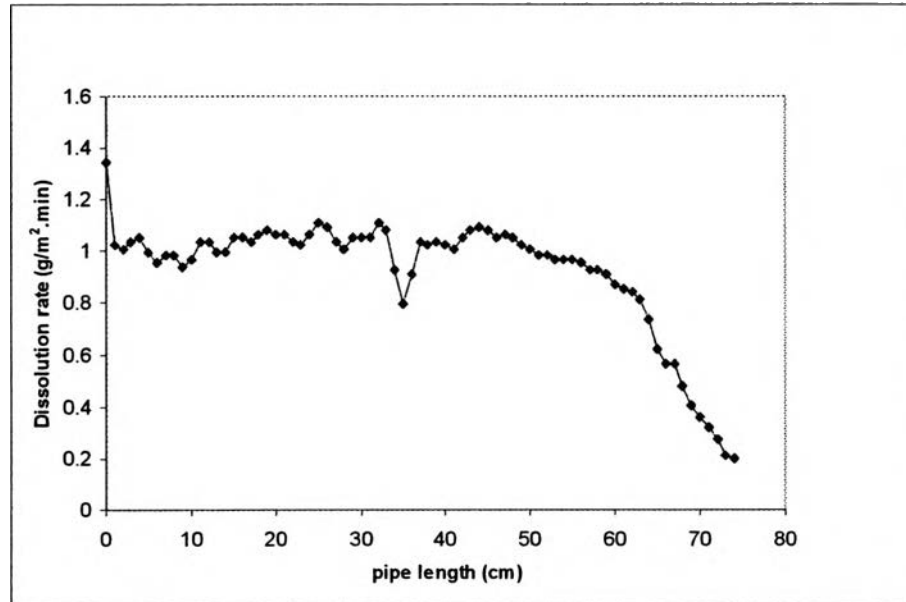


Figure F.15 The dissolution rate profile along the pipe under condition $\text{pH}_{25^\circ\text{C}} 7$, 10°C and 35 LPM (the first run)

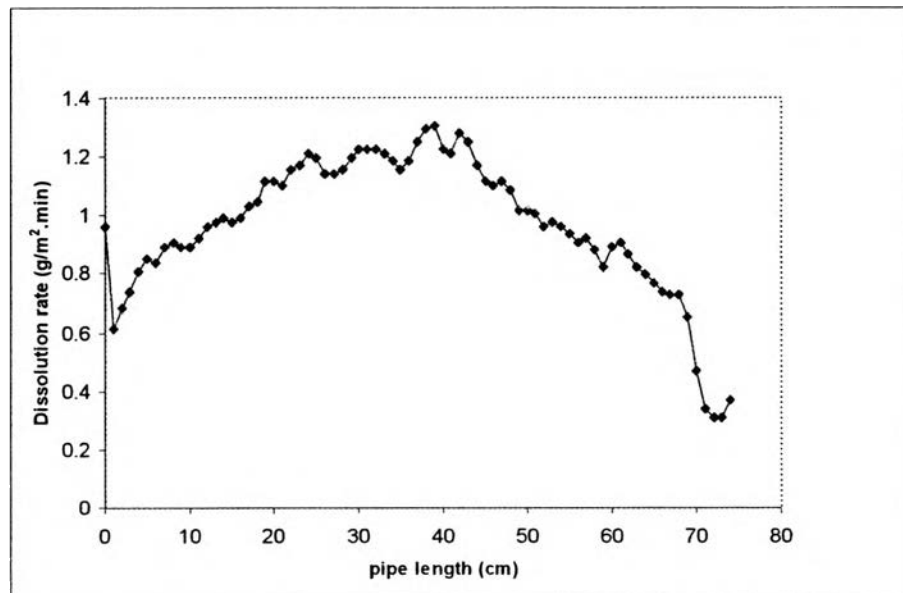


Figure F.16 The dissolution rate profile along the pipe under condition $\text{pH}_{25^\circ\text{C}} 7$, 10°C and 35 LPM (the second run)

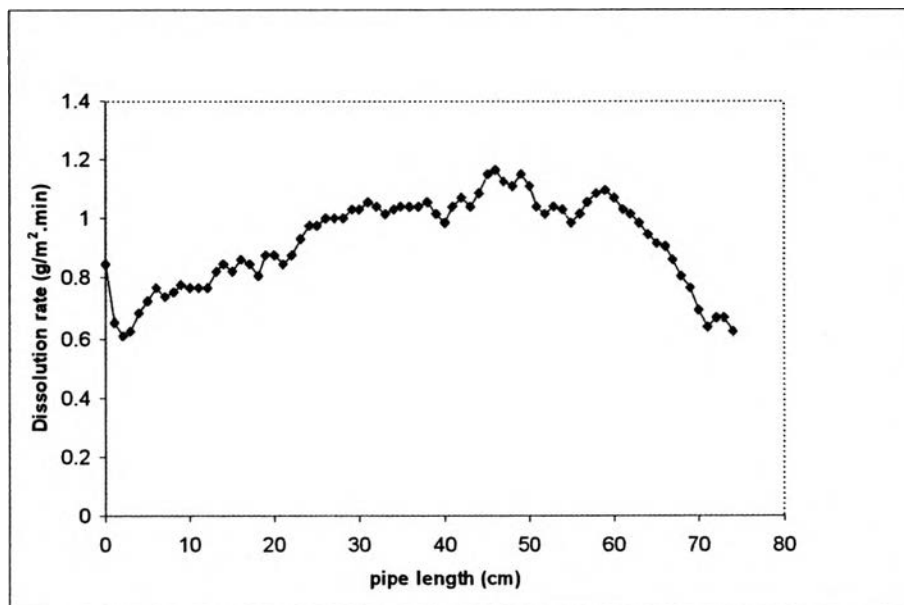


Figure F.17 The dissolution rate profile along the pipe under condition $\text{pH}_{25^\circ\text{C}} 10$, 10°C and 35 LPM (the first run)

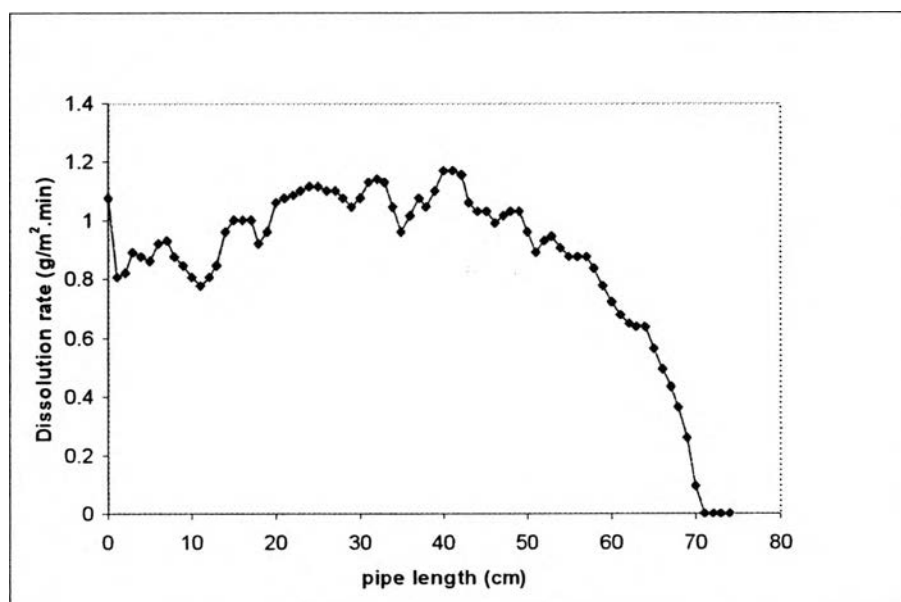


Figure F.18 The dissolution rate profile along the pipe under condition $\text{pH}_{25^\circ\text{C}} 10$, 10°C and 35 LPM (the second run)

F.2 Dissolution Coefficient Along the Pipe and Mass Transfer Coefficient

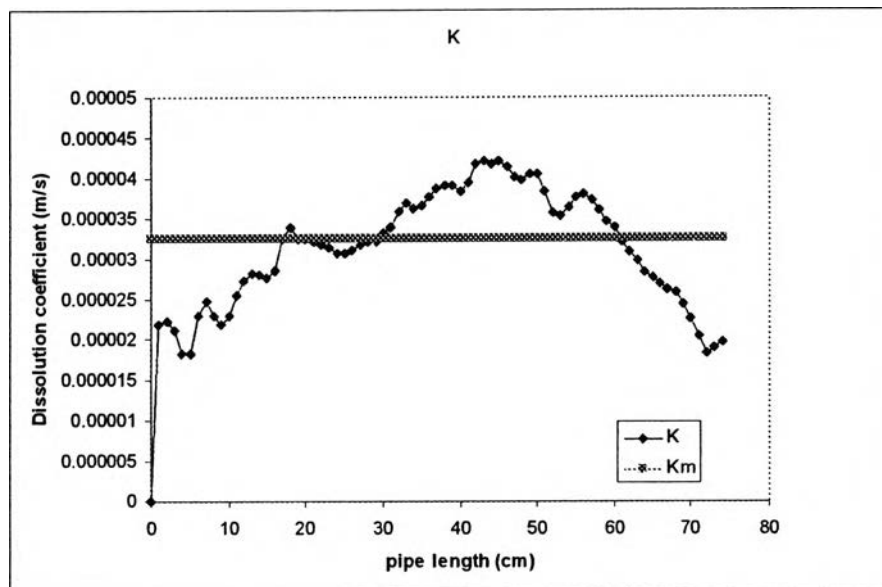


Figure F.19 The dissolution coefficient (K) compared with the mass transfer coefficient (K_m) along the pipe under condition pH_{25°C} 3, 25°C and 25 LPM (the second run)

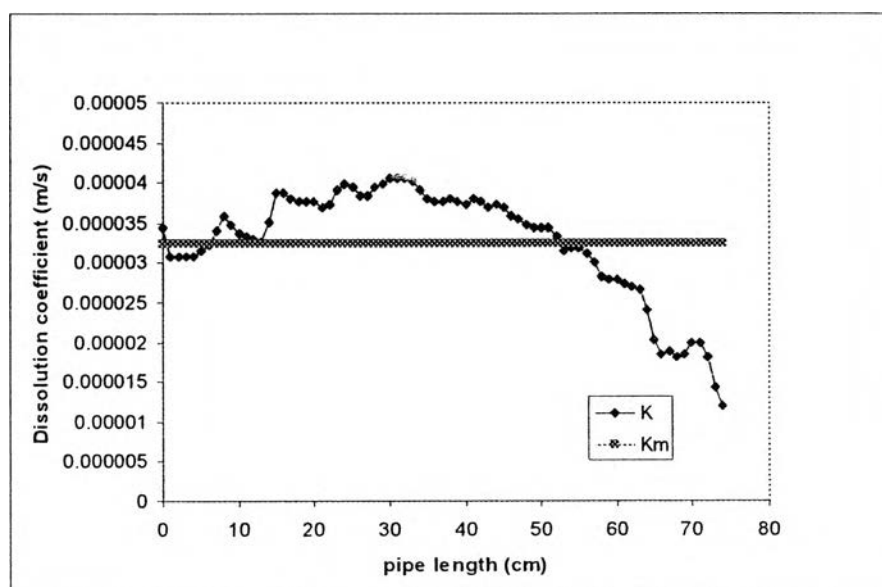


Figure F.20 The dissolution coefficient (K) compared with the mass transfer coefficient (K_m) along the pipe under condition pH_{25°C} 7, 25°C and 25 LPM (the second run)

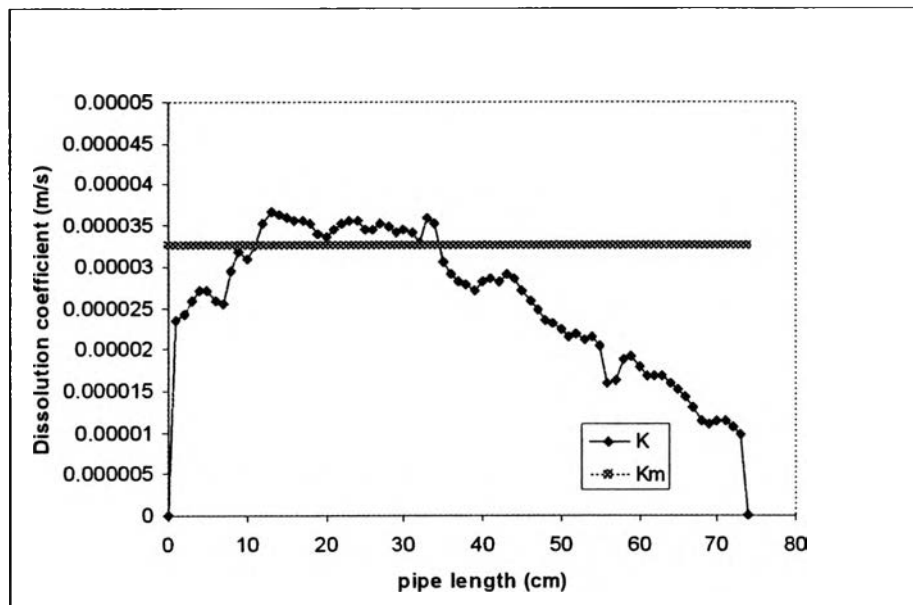


Figure F.21 The dissolution coefficient (K) compared with the mass transfer coefficient (K_m) along the pipe under condition $\text{pH}_{25^\circ\text{C}} 10$, 25°C and 25 LPM (the second run)

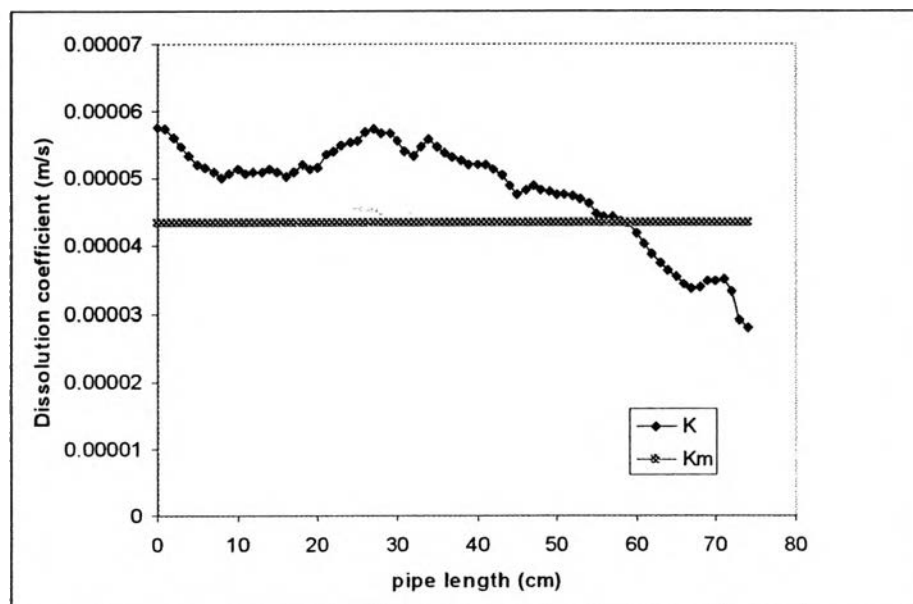


Figure F.22 The dissolution coefficient (K) compared with the mass transfer coefficient (K_m) along the pipe under condition $\text{pH}_{25^\circ\text{C}} 3$, 25°C and 35 LPM (the first run)

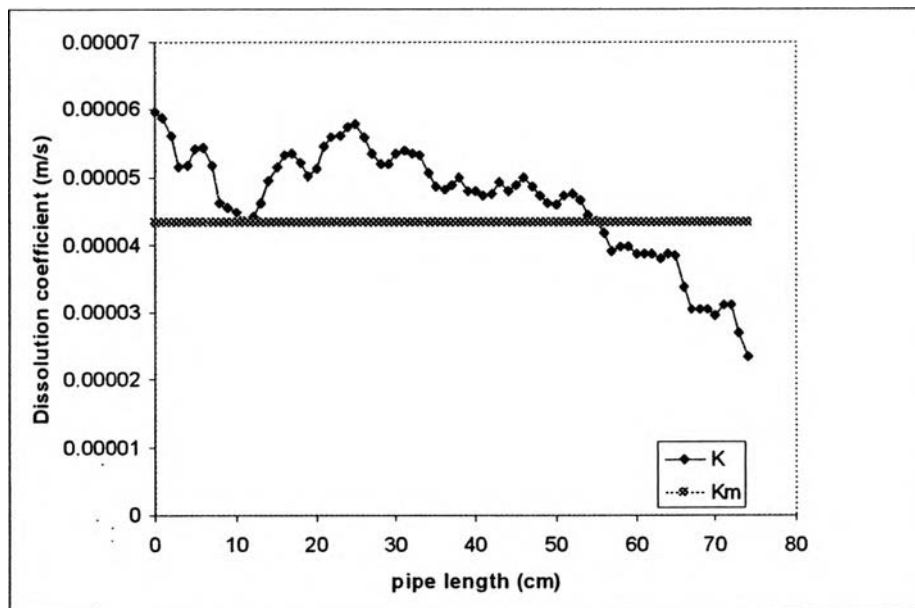


Figure F.23 The dissolution coefficient (K) compared with the mass transfer coefficient (K_m) along the pipe under condition $\text{pH}_{25^\circ\text{C}}$ 3, 25°C and 35 LPM (the second run)

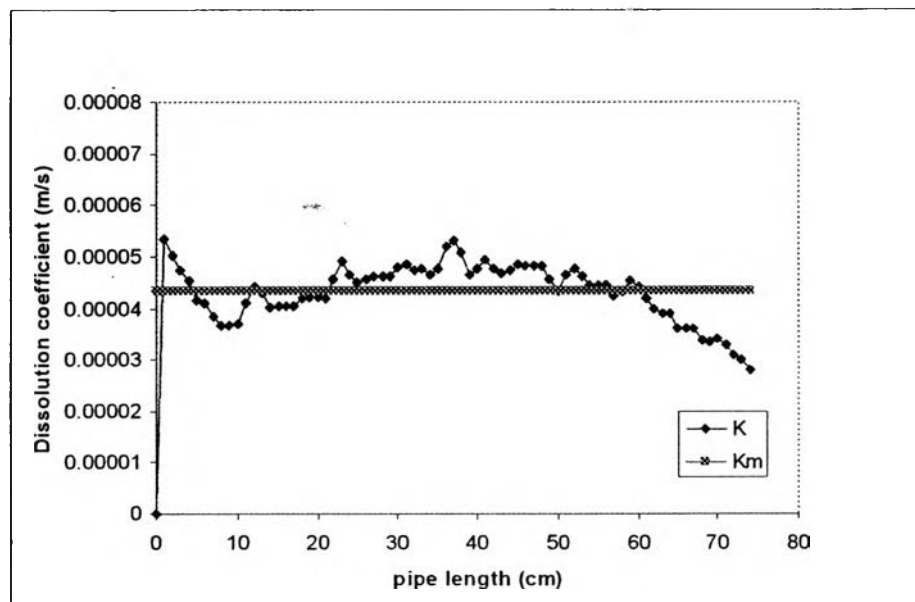


Figure F.24 The dissolution coefficient (K) compared with the mass transfer coefficient (K_m) along the pipe under condition $\text{pH}_{25^\circ\text{C}}$ 7, 25°C and 35 LPM (the first run)

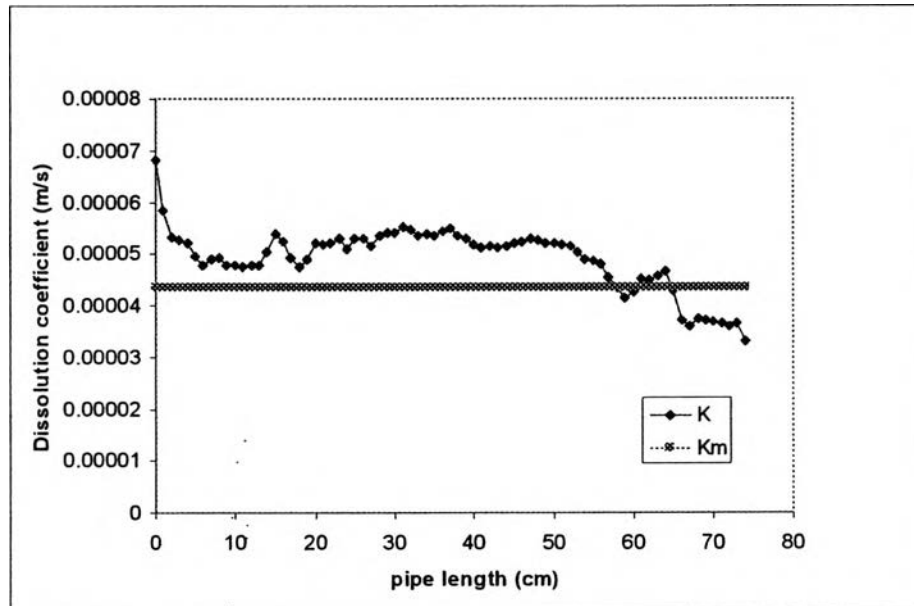


Figure F.25 The dissolution coefficient (K) compared with the mass transfer coefficient (K_m) along the pipe under condition $\text{pH}_{25^\circ\text{C}}$ 7, 25°C and 35 LPM (the second run)

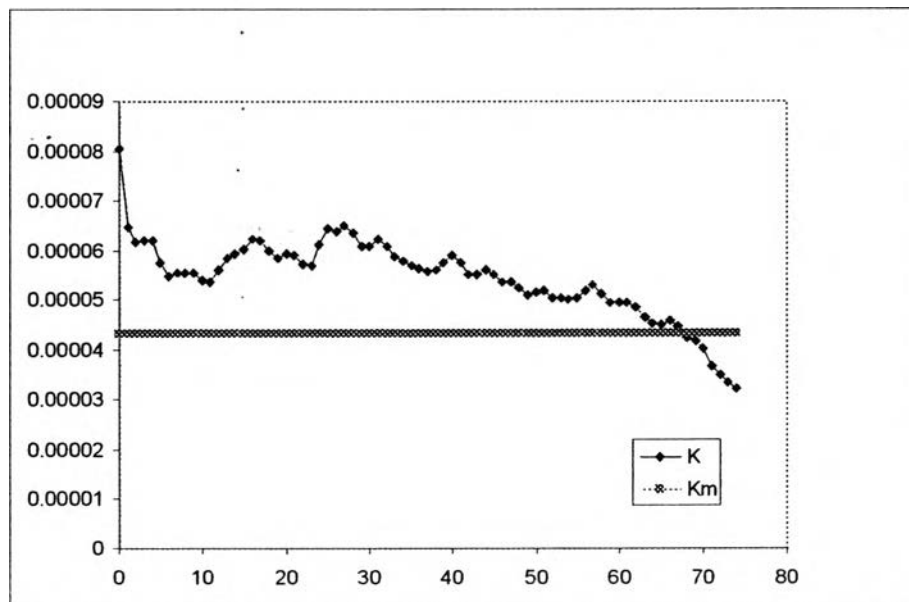


Figure F.26 The dissolution coefficient (K) compared with the mass transfer coefficient (K_m) along the pipe under condition $\text{pH}_{25^\circ\text{C}}$ 10, 25°C and 35 LPM (the first run)

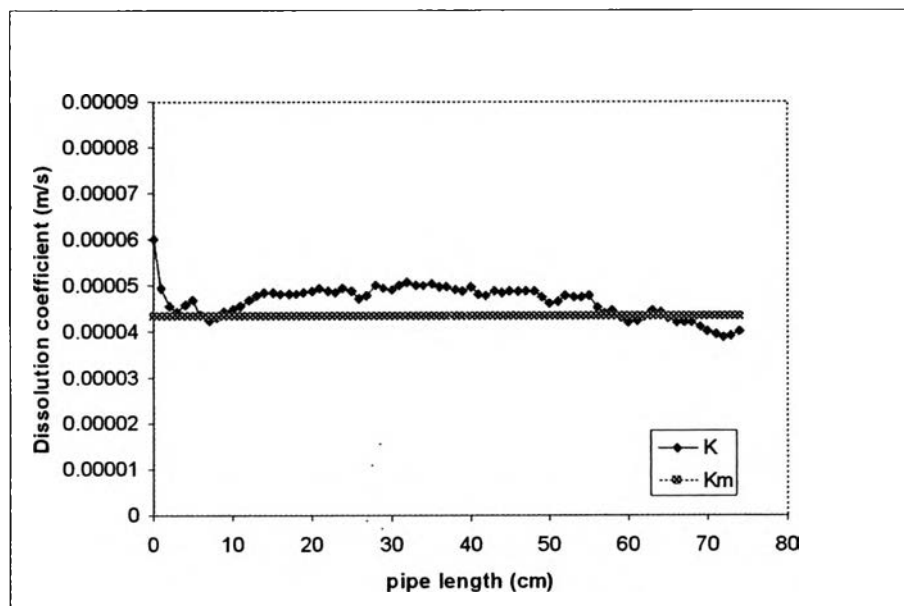


Figure F.27 The dissolution coefficient (K) compared with the mass transfer coefficient (K_m) along the pipe under condition $\text{pH}_{25^\circ\text{C}}$ 10, 25°C and 35 LPM (the second run)

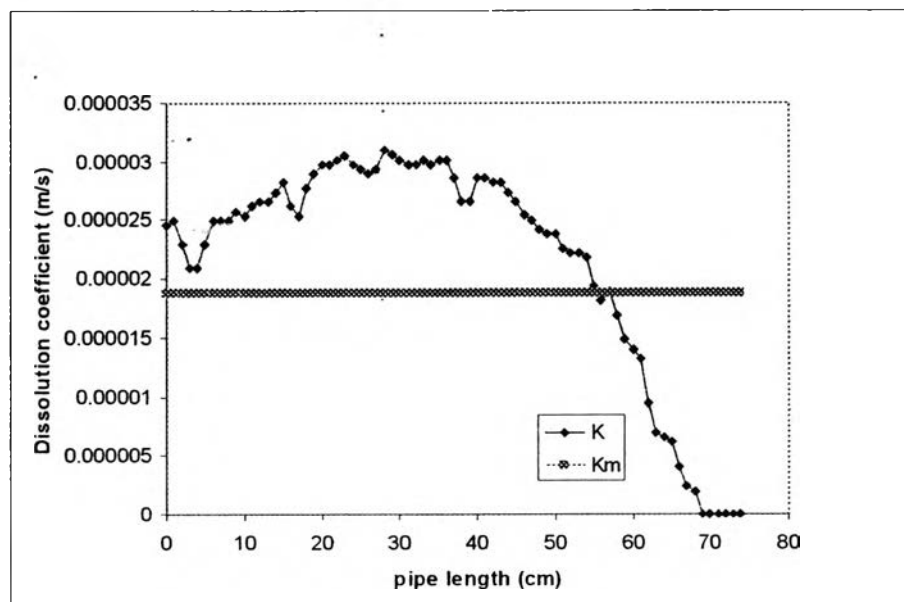


Figure F.28 The dissolution coefficient (K) compared with the mass transfer coefficient (K_m) along the pipe under condition $\text{pH}_{25^\circ\text{C}}$ 3, 10°C and 25 LPM (the second run)

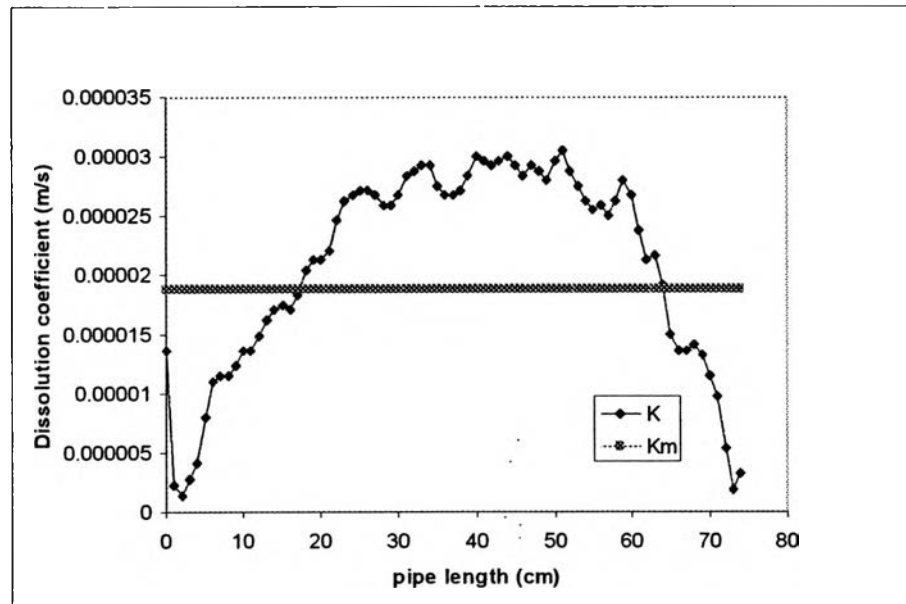


Figure F.29 The dissolution coefficient (K) compared with the mass transfer coefficient (K_m) along the pipe under condition $\text{pH}_{25^\circ\text{C}} 7$, 10°C and 25 LPM (the second run)

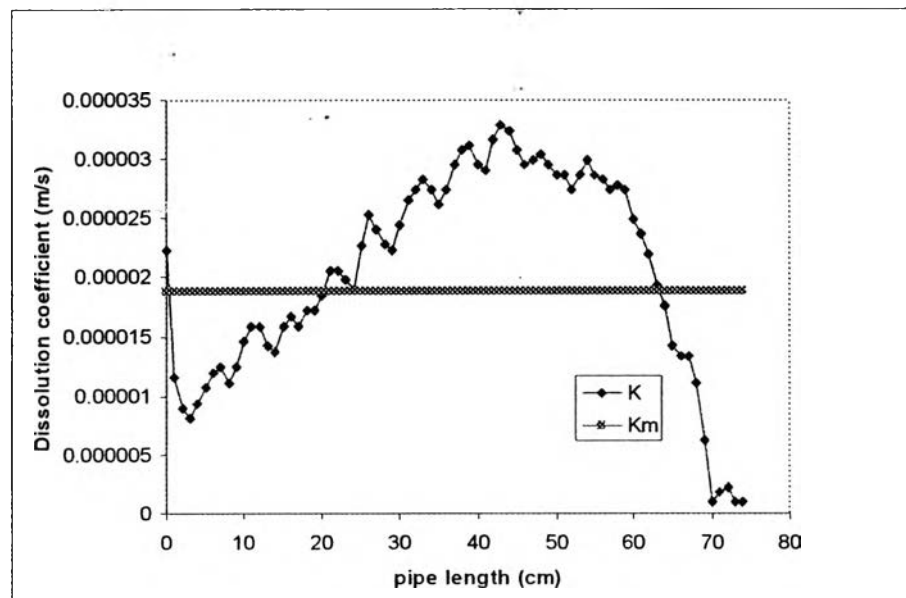


Figure F.30 The dissolution coefficient (K) compared with the mass transfer coefficient (K_m) along the pipe under condition $\text{pH}_{25^\circ\text{C}} 10$, 10°C and 25 LPM (the second run)

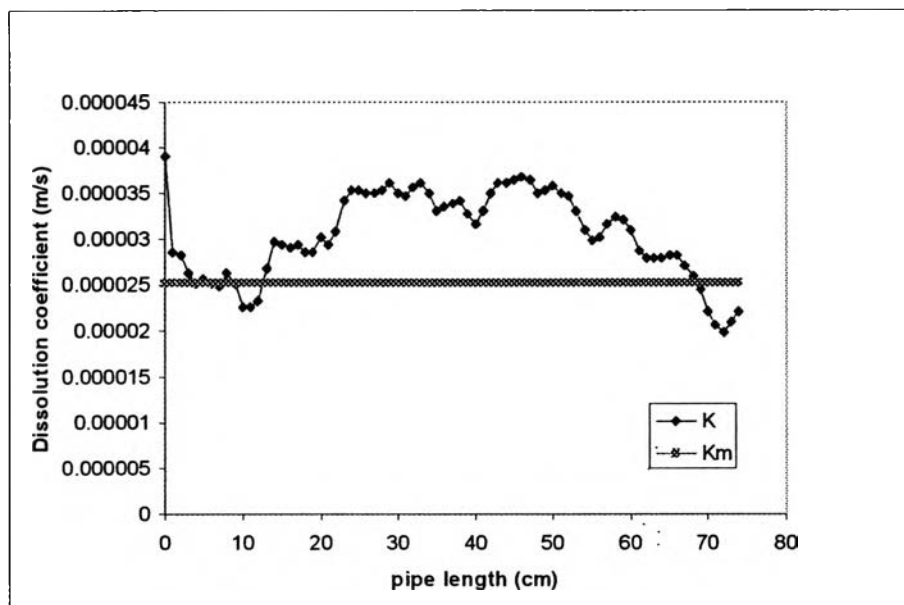


Figure F.31 The dissolution coefficient (K) compared with the mass transfer coefficient (K_m) along the pipe under condition $\text{pH}_{25^\circ\text{C}} 3$, 10°C and 35 LPM (the first run)

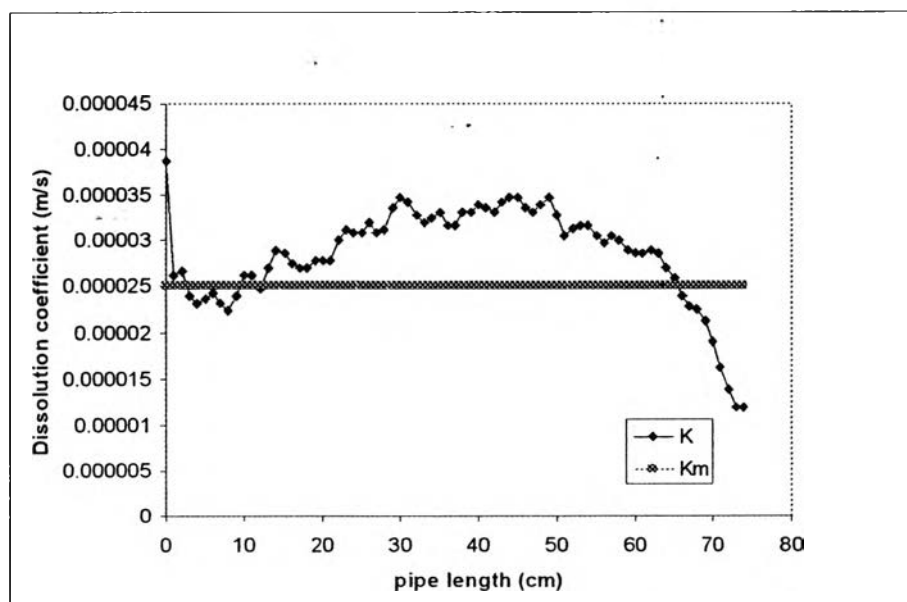


Figure F.32 The dissolution coefficient (K) compared with the mass transfer coefficient (K_m) along the pipe under condition $\text{pH}_{25^\circ\text{C}} 3$, 10°C and 35 LPM (the second run)

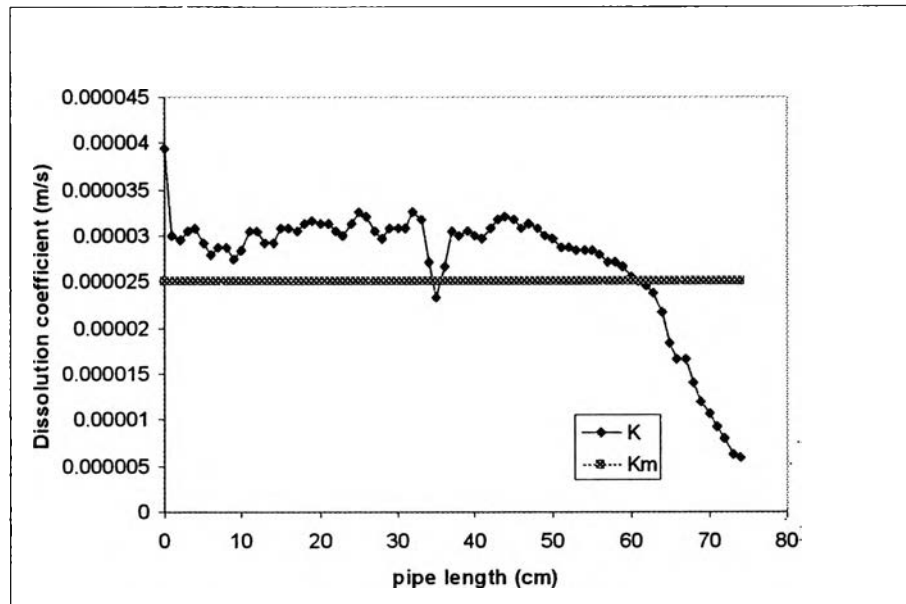


Figure F.33 The dissolution coefficient (K) compared with the mass transfer coefficient (K_m) along the pipe under condition $\text{pH}_{25^\circ\text{C}}$ 7, 10°C and 35 LPM (the first run)

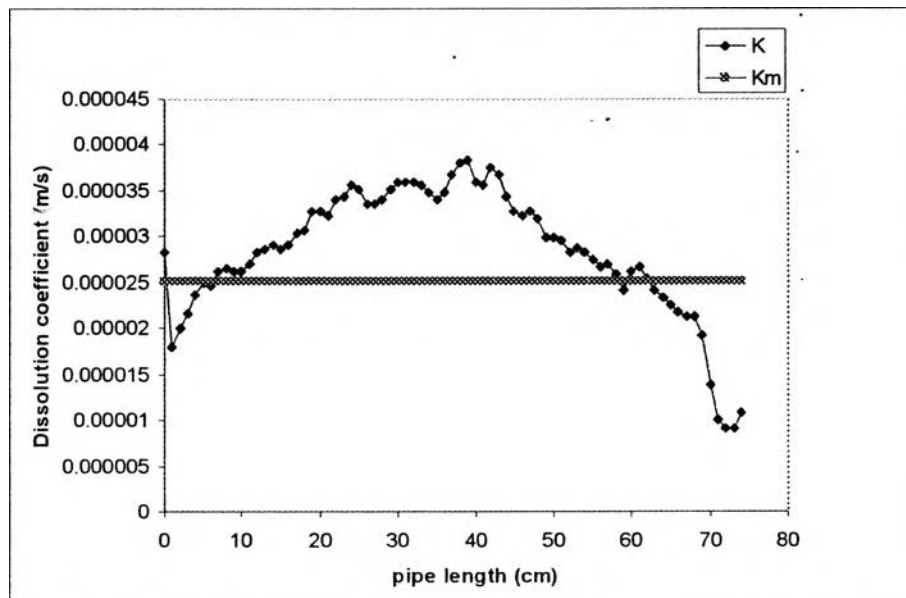


Figure F.34 The dissolution coefficient (K) compared with the mass transfer coefficient (K_m) along the pipe under condition $\text{pH}_{25^\circ\text{C}}$ 7, 10°C and 35 LPM (the second run)

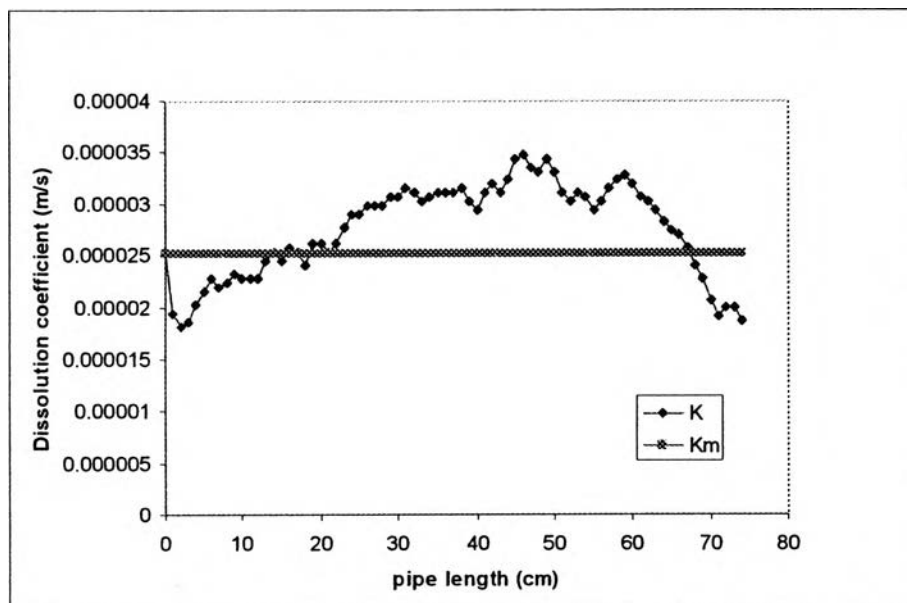


Figure F.35 The dissolution coefficient (K) compared with the mass transfer coefficient (K_m) along the pipe under condition $\text{pH}_{25^\circ\text{C}} 10$, 10°C and 35 LPM (the first run)

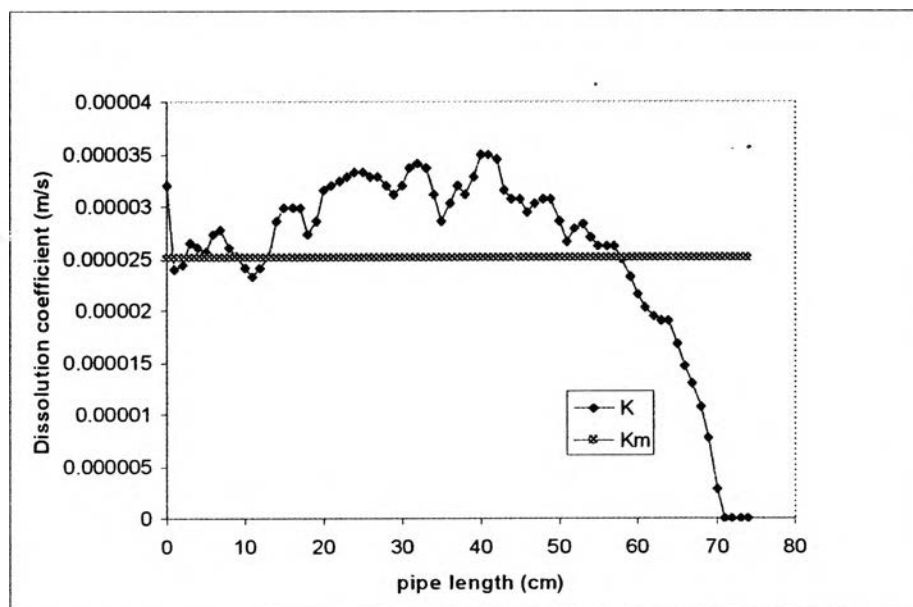


Figure F.36 The dissolution coefficient (K) compared with the mass transfer coefficient (K_m) along the pipe under condition $\text{pH}_{25^\circ\text{C}} 10$, 10°C and 35 LPM (the second run)

Note: The dissolution rate or dissolution coefficient is zero value because the plaster tubes were cut for SEM analysis before measuring the thickness. Therefore, the thickness data at that position could not be found out.

